Tectonophysics 749 (2018) 88–103

Contents lists available at ScienceDirect

Tectonophysics

journal homepage: www.elsevier.com/locate/tecto

The Paleogene arcs of the northern Andes of Colombia and Panama: Insights on plate kinematic implications from new and existing geochemical, geochronological and isotopic data

A. Cardona[a,b,*], S. León[b,c], J.S. Jaramillo[b,d], C. Montes[e], V. Valencia[f], J. Vanegas[g], C. Bustamante[g], S. Echeverri[b,h]

[a] Departamento de Procesos y Energía, Facultad de Minas, Universidad Nacional de Colombia, Medellín, Colombia
[b] Grupo de Investigación en Geología y Geofísica (EGEO), Universidad Nacional de Colombia, Medellín, Colombia
[c] Smithsonian Tropical Research Institute, Balboa, Ancon, Panama
[d] Departamento de Materiales y Minerales, Facultad de Minas, Universidad de Colombia, Medellín, Colombia
[e] Departamento de Física y Geociencias, Universidad del Norte, Barranquilla, Colombia
[f] School of the Environment, Washington State University, Pullman, WA, USA
[g] Departamento de Ciencias de la Tierra, Universidad EAFIT, Medellín, Colombia
[h] Instituto de Geociências, Universidade de São Paulo, São Paulo, Brazil

ARTICLE INFO

Keywords:
Northern Andes
Magmatic arcs
Paleogene
Caribbean plate
Plate kinematics
Central America

ABSTRACT

The northern Andes of Colombia comprise two non-cogenetic Paleogene arcs formed in contrasting geodynamic settings including continental and oceanic domains. New whole-rock geochemistry and isotopic constraints, together with a review of 332 geochemical, 76 isotopic and 204 geochronological data from Paleocene to Eocene volcanic and plutonic rocks exposed in central and western Colombia and Panama, are used to evaluate cause-effect relations between regional plate kinematics and the spatio-temporal distribution of the circum-Caribbean magmatic arcs. Short-lived, ~60–45 Ma arc-like magmatism in the Central Cordillera of Colombia was emplaced in a thickened continental crust due to the oblique subduction of the Caribbean oceanic plate underneath South America, as suggested by the high Sr/Y ratios. Conversely, the Panama Arc, and its poorly explored extension in the northwestern segment of the Western Cordillera of Colombia document a major phase of tholeiitic to calc-alkaline arc magmatism between ~71 Ma and ~34 Ma, mostly derived from a hydrated mantle wedge, and emplaced in an oceanic plateau crust. This arc record a major phase of magmatic activity between 40 Ma and 50 Ma that can be associated to changes in the convergence direction and subduction rates of the Farallon plate.

Farther to the south, in the Pacific region of Colombia, Eocene arc-related rocks from the Timbiqui Complex show a geochemical signature that suggests a magmatic origin from melting of both a subduction-modified mantle and lower tectonically thickened crust. A possible interpretation for the Pacific and Western Colombia-Panama Arc systems, and its analogous in Ecuador, recall an Aleutian-type convergent margin in which the continental arc laterally switches to a purely oceanic system along the trailing edge of the Caribbean plate as consequence of eastward subduction of the Farallon plate.

1. Introduction

The spatial distribution and the composition of arc-related magmatism are the product of upper- and lower-plate processes, and consequence of subduction dynamics such as convergence geometry, lower plate thermal state and composition, slab dip-angle, upper plate thickness and deformational evolution (Ducea et al., 2015; Gazel et al., 2015; Kay et al., 2005; Mamani et al., 2010; Wegner et al., 2011; Wörner et al., 2009). Such patterns are expected to vary through time and therefore, can be used to reconstruct the long-term evolution of magmatic arcs and refine paleogeographic models in margins, which have been shaped by protracted subduction.

In the northern Andes of Colombia and Central America, contrasting Paleocene-Eocene magmatic arcs have been documented. These, mainly include a discontinuous belt exposed along the Central Cordillera and the Caribbean Region of Colombia (Bayona et al., 2012; Bustamante et al.,

* Corresponding author at: Departamento de Procesos y Energía, Facultad de Minas, Universidad Nacional de Colombia, Medellín, Carrera 80 # 65 – 223, Colombia.
E-mail address: agcardonamo@unal.edu.co (A. Cardona).

https://doi.org/10.1016/j.tecto.2018.10.032
Received 31 May 2018; Received in revised form 19 October 2018; Accepted 30 October 2018
Available online 06 November 2018

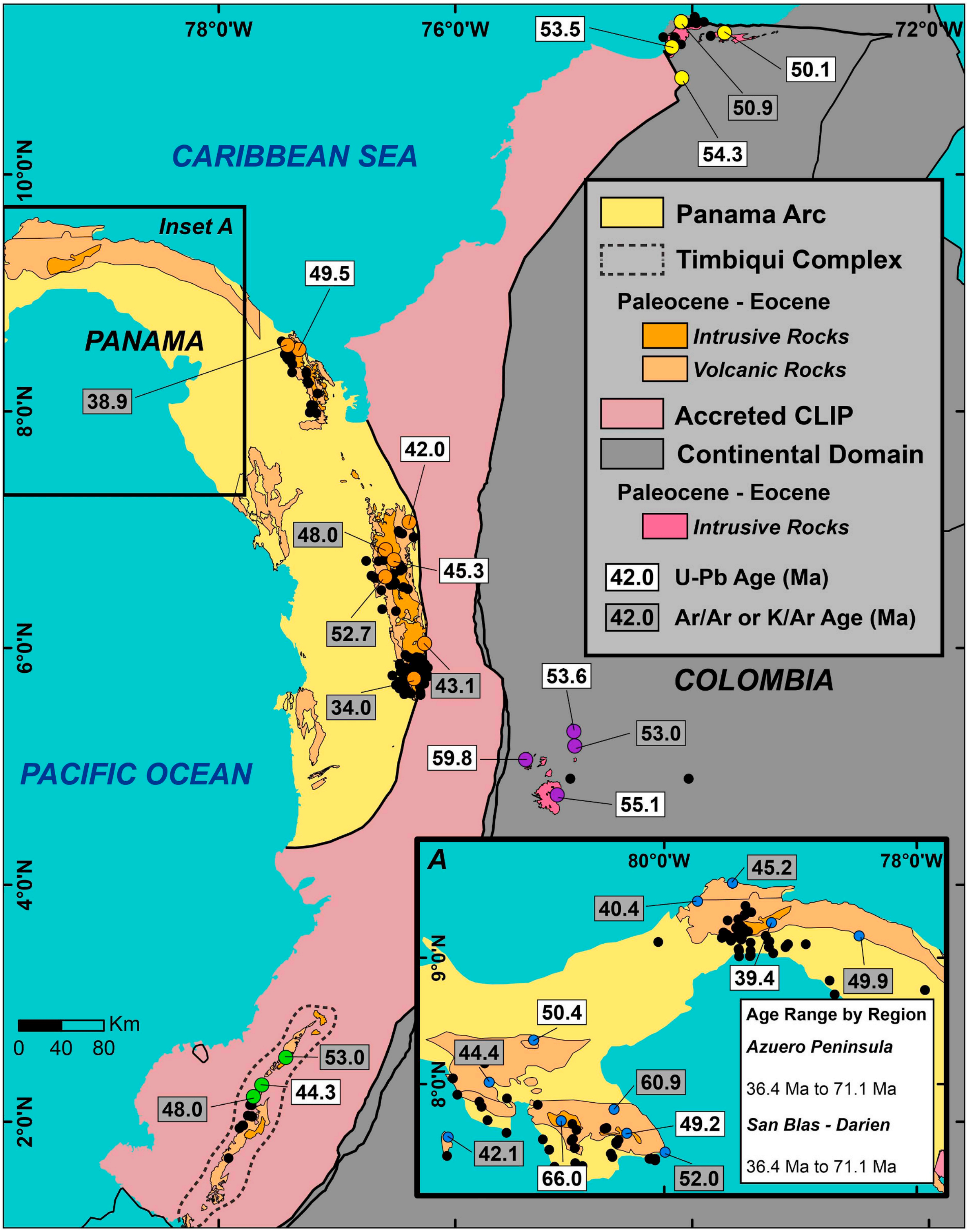

Fig. 1. Regional geological map showing the spatial distribution of Paleocene-Eocene units discussed in text, compiled geochemical samples (black dots), and selected geochronological data from the compiled database (blue = oceanic Panamanian arc, orange = oceanic Colombian arc, green = Timbiqui Complex, purple = Central Cordillera continental arc, yellow = Caribbean Region continental arc; not all 204 samples were plotted in order to avoid saturation). Inset A shows the Panamanian units. Elaborated after Lissinna (2005) and Gómez-Tapias et al. (2015). Complete tables of the used geochronological and geochemical databases can be found in Supplementary material Tables S1 and S2. (For interpretation of the references to color in this figure legend, the reader is referred to the web version of this article.)

2017; Cardona et al., 2011a, 2011b, 2014), and an apparently continuous domain exposed in the western flank of the Western Cordillera and the Urabá region of Colombia (Fig. 1). The latter extends towards the San Blas Range, the Azuero-Soná peninsula and Central Panama, and is included within the Panama Arc (Aspden et al., 1987; Lissinna, 2005; Montes et al., 2015; Wegner et al., 2011; Whattam et al., 2012). Moreover, a poorly exposed arc fragment in the southwestern Pacific region of Colombia has been also reported (McCourt et al., 1990a, 1990b).

The tectonic implications of these arcs in the Central Cordillera, as well as its relation with the eastern foreland basins of Colombia and the subduction of the Caribbean plate underneath South American have already been reviewed in Bayona et al. (2012), Bustamante et al. (2017), and Cardona et al. (2011a, 2011b, 2014). However, the tectono-magmatic record in the Western Cordillera has been barely studied (Kerr et al., 1997; Montes et al., 2015; Villagómez et al., 2011), with most of the discussions limited to the temporal similarities with the coeval Panamanian rocks. There, a more extensive geochronological and geochemical database is available, which has been recently discussed in terms of long-term arc evolution (Buchs et al., 2010; Farris et al., 2017; Lidiak and Jolly, 1996; Lissinna, 2005; Montes et al., 2012a, 2012b; Ramírez et al., 2016; Wegner et al., 2011; Whattam et al., 2012; Wörner et al., 2009). Moreover, the geodynamic significance and origin of coeval arc-related rocks exposed in the Western Cordillera of Ecuador (e.g. Macuchi Arc), also still controversial (e.g. Chiaradia, 2009; Hughes and Pilatasig, 2002; Vallejo et al., 2009).

In this contribution, we present a review of published geochronological, geochemical and isotopic results from Paleogene rocks of Panama, the Central and Western Cordilleras and the southwestern Pacific region of Colombia. We additionally present new geochemical and isotopic (Sr-Nd-Pb-Hf) data from plutonic and volcanic rocks of the Western Cordillera, together with whole rock Sr-Nd results from plutonic rocks of Central Panama and the Azuero region. The spatio-temporal and compositional characteristics of the Paleogene arc-related rocks from Panama and Colombia were influenced by changes in plate convergence obliquity and the velocity of the subducting Farallon and Caribbean plates, triggered by the collision and subduction of the Caribbean plate margins with the Americas.

2. Geological setting

The transition between the Cretaceous and the early Paleogene in the Andes of Colombia is marked by the construction of a magmatic arc following an oblique arc-continent collision between the leading edge of the Caribbean plate and the continental margin (Bayona et al., 2012; Bustamante et al., 2017; Cardona et al., 2011a, 2011b). The Late Cretaceous – Paleocene arc-related units are exposed as a series of elongated plutonic bodies of stock and batholith size, mainly granodioritic and quartzdioritic in composition, intruding Triassic, Jurassic and Cretaceous metamorphic rocks of the Central Cordillera, the Sierra Nevada de Santa Marta and the Guajira Ranges (Bayona et al., 2012; Bustamante et al., 2017; Cardona et al., 2011a, 2011b, 2014). Such magmatism is characterized by a well-defined arc related geochemical signature that has been related to the subduction of the Caribbean plate underneath the South American margin between ~60–45 Ma, and whose distribution could extend as far as 400 km inboard (Bayona et al., 2012; Bustamante et al., 2017; Cardona et al., 2011a, 2011b, 2014).

In the Western Cordillera of Colombia, Eocene intermediate plutonic rocks with arc-related geochemical signature have been mostly included in the Mande and Acandi batholiths, which are related to Paleogene volcanic rocks of the Santa Cecilia-La Equis Complex or the so-called Dabeiba Arc (Buchely et al., 2009; González and Londoño, 2002; Kerr et al., 1997). For both, the plutonic and volcanic rocks, zircon U-Pb as well as Ar/Ar and K/Ar ages ranging between ~59 and 39 Ma have been reported. Volcanic and plutonic rocks across the Colombia – Panama boundary in the San Blas Range, Central Panama (Chagres-Bayano Complex), and Azuero-Soná Peninsula, are also characterized by an oceanic arc origin, with crystallization ages between 70 Ma and 36 Ma. Such arc magmatism that apparently initiated at ca. 71–66 Ma or earlier (Buchs et al., 2010; Montes et al., 2015; Wegner et al., 2011), intrudes and overlies Cretaceous plateau-related rocks (reviews in Buchs et al., 2010; Lissinna, 2005; Wegner et al., 2011).

Along the Pacific region of southern Colombia, several agglomerates, andesites and volcano-clastic rocks, as well as minor plutonic units Eocene in age, have been included in the Timbiqui arc Complex (ANH-GRP, 2011; Annells et al., 1988; Barbosa-Camacho, 2003; McCourt et al., 1990a, 1990b). The tectono-magmatic origin of these rocks, however, has been barely explored, being considered as either a continental arc (Pindell and Kennan, 2009) or as an allochthonous arc that was accreted to the continental margin by the Oligocene (Echeverri et al., 2015a).

3. Methods

We compiled 332 geochemical, 76 isotopic and 204 U-Pb, Ar/Ar, and K/Ar geochronological analyses available from published research papers and mapping reports of the Colombian Geological Survey. We only included samples for which the abundances of major oxides, as well as trace and rare earth elements were available. Additionally, we present new geochemical (18 samples) and isotopic data (Sr-Nd-Hf-Pb; 71 analyses) obtained from the Norcasia and Hatillo Stocks, the Acandi Batholith and the Santa Cecilia-La Equis Complex, as well as new Sr-Nd isotopic data from Central Panama and Azuero-Soná granitoids. Compiled and new geochemical, geochronological and isotopic data are presented in Supplementary material Tables S1 to S3. Our sampling targeted mostly sequences of the oceanic Panama Arc in Colombia, since its tectono-magmatic significance, at least in a regional framework, is less understood than that of the continental domain.

3.1. Whole rock geochemistry

Whole-rock geochemical analyses of 18 samples from the Acandi Batholith and the Santa Cecilia-La Equis Complex were obtained by inductively coupled plasma-mass spectrometry (ICP-MS) at Acme Analytical Laboratories Ltd. in Vancouver, Canada. For each sample, a 0.2 g of rock powder was placed into a graphite crucible and mixed with 1.5 g of $LiBO_2$ flux. The crucibles were placed in an oven and heated to 1050 °C for 15 min. The molten sample was dissolved in 5% HNO_3. Calibration standards and reagent blanks were added and the solutions were aspirated into an ICP emission spectrometer. Detection limits for the major elements vary between 0.001% and 0.004%, whereas trace elements values are around 0.1 ppm, whereas rare earth elements have lower detection limits between 0.01 and 0.05 ppm. Results from the geochemical analyses were handled and processed using the software GCD Kit 4.1 (Janoušek et al., 2006). In Fig. 4A and B, we report the distribution and mean values of both Sr/Y and $(La/Yb)_N$ values for each analyzed tectono-magmatic unit. These values were estimated after running a basic outliers analysis by using R 3.2.1, which were used to estimate crustal thickness in order to avoid anomalous values that might be related to altered samples (Chiaradia, 2015).

3.2. Whole rock and zircon Sr-Nd-Pb-Hf isotopes

Sr, Nd and Pb whole rock isotopic analysis were conducted at the University of Arizona. Rb, Sr, Sm, and Nd were determined by isotope dilution following the methodology described by Ducea et al. (2002). The Sr isotopic ratios of standards and samples were normalized to $^{86}Sr/^{88}Sr = 0.1194$, whereas the Nd isotopic ratios were normalized to $^{146}Nd/^{144}Nd = 0.7219$. Analyses were performed on a multi-collector inductively coupled plasma mass spectrometer (MC-ICP-MS). Pb isotopic analysis follows Wetmore and Ducea (2011). Washes from the cation column separation were used for separating Pb. Isotopic analyses were conducted on a GV Instruments (Hudson, NH, USA) MC-ICP-MS. All results were Hg-corrected and empirically normalized to Tl by using an exponential law correction. To correct for machine and interlaboratory bias, all results were normalized to values reported by Galer and Abouchami (2004) for the National Bureau of Standards (NBS)-981 standard ($^{206}Pb/^{204}Pb = 16.9405$, $^{207}Pb/^{204}Pb = 15.4963$, and $^{208}Pb/^{204}Pb = 36.7219$). The internal error reflects the reproducibility of the measurements on individual samples, whereas external errors are derived from long-term reproducibility of NBS-981 Pb standard and result in part from the mass bias effects within the instrument. In all cases, external error exceeds the internal errors and is reported below. External errors associated with each Pb isotopic ratio are as follows: $^{206}Pb/^{204}Pb = 0.028\%$, $^{207}Pb/^{204}Pb = 0.028\%$ and $^{208}Pb/^{204}Pb = 0.031\%$.

Zircon Hf isotope geochemistry conducted at the Geoanalytical Lab of the Washington State University, using a ThermoFinnigan Neptune™ MC-ICP-MS equipped with 9 faraday collectors interfaced with a New Wave™ 213 nm UP Nd-YAG laser. The laser was operated at a pulse of rate 10 Hz and a fluence of 10–12 J/cm2. Laser spot size was 30 μm. Carrier gas consisted of purified He plus small quantities of N2 to minimize oxide formation and increase Hf sensitivity. The total Hf signal achieved was between 2 and 6 V. The data were acquired in static mode with 60-second integrations. Details of analytical procedures and data treatment are after (DuFrane et al., 2007; Vervoort et al., 2004). For the Hf-depleted mantle model ages (Hf TDM), we used $^{176}Hf/^{177}Hf$ and $^{176}Lu/^{177}Hf$ for the individual zircon samples to determine their initial $^{176}Hf/^{177}Hf$ ratios at their crystallization ages. Projection back from zircon crystallization was calculated using a present value of 0.0093 for $^{176}Lu/^{177}Hf$ crust (Amelin et al., 2000; Vervoort and Patchett, 1996). The depleted mantle Hf evolution curve was calculated from present-day depleted mantle values of $^{176}Hf/^{177}Hf$ DM (0) = 0.283225 and $^{176}Lu/^{177}Hf$ DM(0) = 0.038512 (Vervoort and Blichert-Toft, 1999).

4. Results

In the following section, we integrate published results with the newly obtained data from several localities of Colombia and Panama, in order to constitute a strong geochronological, isotopic and geochemical framework for the Paleogene volcanic and plutonic rocks of the region. Results are presented separately for each domain and are subsequently discussed in regarding their geochemical-isotopic features. The discussion will be limited to the Late Cretaceous – Eocene record, since younger magmatic episodes have been more widely discussed in the context of the Farallon plate fragmentation and the collision of the Panama Arc with NW South America (Farris et al., 2011; León et al., 2018; Montes et al., 2012a, 2012b; Ramírez et al., 2016; Schütte et al., 2010; Wegner et al., 2011; Wörner et al., 2009).

4.1. Continental arc of the Central Cordillera and the Caribbean Region

Paleogene arc-related magmatic rocks in the Central Cordillera and the Caribbean region of Colombia include different plutonic bodies of stock and batholith size such as Manizales, Hatillo, Norcasia and Parashi stocks, and Antioquia, Sonsón, El Bosque, Santa Bárbara and Santa Marta batholiths (Bayona et al., 2012; Bustamante et al., 2017; Cardona et al., 2011a, 2011b, 2014; Leal-Mejía, 2011; Ordoñez et al., 2001; Ordoñez-Carmona et al., 2011). These rocks intrude the Triassic, Jurassic and Cretaceous metamorphic rocks from the central and eastern flanks of the Central Cordillera (Fig. 1; review in Bustamante et al., 2017). Compositionally, they vary between gabbros and granodiorites (Fig. 2A), and a well-defined transitional to calc-alkaline magmatic affinity as observed in the AFM diagram (Fig. 2B), as well as in the Zr/Y vs. Th/Yb diagram (see Fig. S1; Ross and Bédard, 2009). Although we attempted to calculate the tholeiitic index (THI; Zimmer et al., 2010), these continental rocks are characterized by Mg values out of the range allowed for such calculation, probably linked to their strong crustal input.

Published data show that SiO_2 from some of the plutons negatively correlate with TiO_2, Al_2O_3, MgO, CaO, and Fe_2O_3, but show a slightly defined positive correlation with K_2O, which is characteristic of a magmatic differentiation trend (Fig. 3).

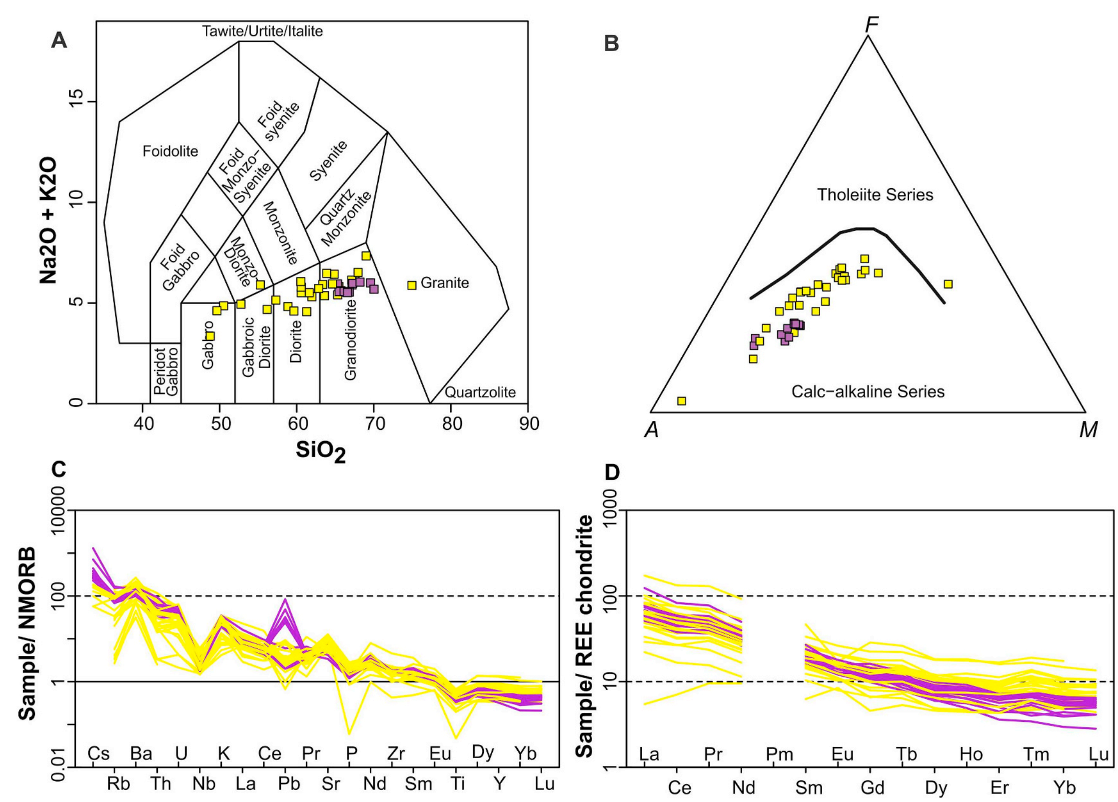

Fig. 2. Classification and spider diagrams of Eocene continental arc-related rocks. A) TAS diagram after Middlemost (1994); B) AFM diagram after Irvine and Baragar (1971); C) Multi-elemental diagram normalized to NMORB after Sun and McDonough (1989); D) REE spider diagram normalized after chondrite values of Nakamura (1974). In purple are samples from the Central Cordillera; yellow from granitoids of the Caribbean region. (For interpretation of the references to color in this figure legend, the reader is referred to the web version of this article.)

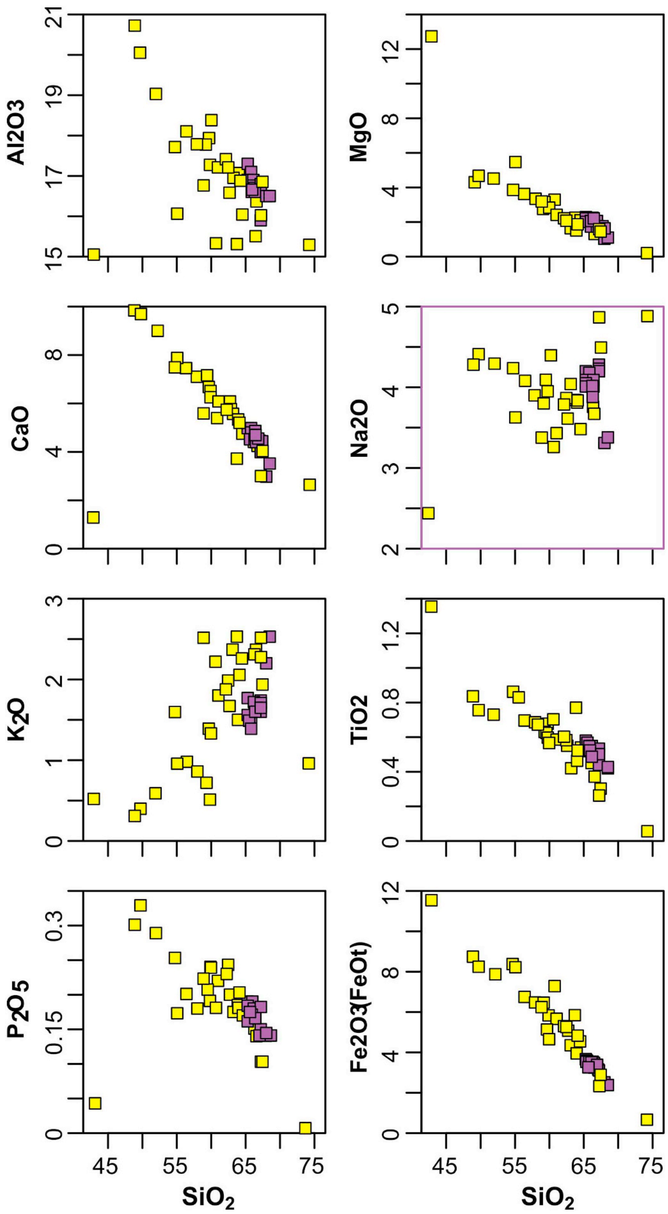

Fig. 3. Harker diagrams showing the relation of major oxides for samples from the Paleogene continental arc-related rocks. Color are the same as in Fig. 2. (For interpretation of the references to color in this figure legend, the reader is referred to the web version of this article.)

Multi-elemental plots normalized to N-MORB (Sun and McDonough, 1989) show well-defined negative Nb and Ti anomalies and enrichment in Large Ion Lithophile Elements (LILE) such as Th, Ba and K (Fig. 2C). The rare earth elements (REE) normalized to the chondrite composition of Nakamura (1974), are characterized by enrichment in the Light Rare Earth Elements (LREE) and depletion of the High Rare Earth Elements (HREE; Fig. 2D). The plutonic rocks present Sr/Y ratios ranging from 21 to 74 which, with a mean value of 39 (Fig. 4A), which is characteristic of melting/differentiation in mid- to high-pressure conditions in the amphibole and garnet stability fields (reviews in Cardona et al., 2014; Bustamante et al., 2017). Furthermore, compiled samples yielded a mean $(La/Yb)_N$ ratio of 3.6 (Fig. 4B).

Published Sr-Nd-Pb whole rock isotopes also show a mixture of radiogenic to juvenile values, with $^{87}Sr/^{86}Sr_{(i)}$ varying between 0.7031 and 0.7107, and $^{143}Nd/^{144}Nd_{(i)}$ from 0.512020 to 0.512735 with $\varepsilon Nd_{(i)}$ values between −10.7 and 3.3. The $^{206}Pb/^{204}Pb$ spans from 18.764 to 18.978, $^{207}Pb/^{204}Pb$ between 15.575 and 15.660, and 208/204 Pb from 38.656 to 38.870 (Fig. 7; Bustamante et al., 2017; Leal-Mejía, 2011; McCourt et al., 1984). We present new zircon Hf isotopic results from two samples including the Hatillo Stock (Sample MLH-1) and Norcasia Stock (Sample MLN-1). Their initial $^{176}Hf/^{177}Hf_{(i)}$ ratio varies between 0.282787 and 0.282946 with $\varepsilon Hf_{(i)}$ between 1.5 and 6.9 (Fig. 8). Bustamante et al. (2017) obtained both similar and more radiogenic Hf isotopes on the Hatillo stock and El Bosque batholiths, which together with our new results suggest the presence of heterogeneous radiogenic continental and juvenile mantle sources (Fig. 8).

4.2. Oceanic Panama Arc

The Panama Arc is an intra-oceanic system whose southwestern edge collided with the northwestern margin of South America during the Neogene or probably earlier (Coates et al., 2004; Duque-Caro, 1990; León et al., 2018; Montes et al., 2015; Pindell and Kennan, 2009). This episode is interpreted as a major tectonic event with primary influence on the north Andean mountain building, and as a first-order control mechanism on the Isthmus closure and the subsequent changes in the global environmental, ecological and oceanographic configuration (Jaramillo et al., 2017; Montes et al., 2015; O'Dea et al., 2016). The tectonic limit between these two domains is marked by the Uramita Fault Zone (UFZ, Duque-Caro, 1990), which is patchily covered by middle Miocene or older sequences with a mixed provenance including detritus from both the Panamian and South-American terranes (León et al., 2018). The suture zone is sealed by ca. 12 Ma arc-related magmatic rocks, which mark the transition from collisional tectonics to the subduction of the Nazca plate underneath South America (León et al., 2018; Rodríguez and Zapata, 2012; Wagner et al., 2017; Zapata and Rodríguez, 2011).

Whattam and Stern (2015) attempted to geodinamically correlate the magmatic units of northwestern South-America and Central America, mainly focusing on Cretaceous units, however, scarce attempts have been done for arc-related Paleocene – Eocene rocks regarding their temporal and compositional features (Montes et al., 2015); in this section, we separately describe each domain to further summarize and discuss the more relevant features.

4.2.1. Panamanian volcanic and plutonic rocks

Paleogene arc-related volcanic rocks have been identified in the San Blas and Darien Regions, Central Panama and the Azuero Peninsula (reviews in Buchs et al., 2010; Coates et al., 2004; Lissinna, 2005; Maury et al., 1995; Montes et al., 2012a, 2012b; Wegner et al., 2011). Volcanic and plutonic rocks are locally deformed and include intercalations of basaltic-andesites to rhyolites, and gabbro-diorite to tonalites, respectively. Volcanics also include andesitic lava, as well as pyroclastic and volcano-clastic rocks (Buchs et al., 2010; Maury et al., 1995; Montes et al., 2012a, 2012b; Wörner et al., 2009). Basaltic pillow-lava is present in minor proportion and is particularly restricted to the lower stratigraphic levels (Buchs et al., 2010; Corral et al., 2016; Montes et al., 2012a, 2012b).

Published K-Ar and Ar-Ar ages obtained from intermediate to acid volcanic rocks, as well as U-Pb ages from plutonic units, have yielded ages between ~71 Ma and ~34 Ma which are related to the magmatic crystallization (see Supplementary material Table S2 for references).

The arc-related rocks from Panama show a dominant basic-intermediate composition, with rare acidic units, including basalts to rhyolites and their plutonic equivalents (Fig. 5A). Both tholeiitic and calc-alkaline trends are defined in the AFM diagram (Fig. 5B), as well as in the Zr/Y vs. Th/Yb diagram (see Fig. S1; Ross and Bédard, 2009). The THI was calculated for 112 samples from the Panama Arc, including the Panamanian and Colombian rocks, which met the FeO and Mg criteria (Zimmer et al., 2010). Alike in the AFM and Zr/Y vs. Th/Yb diagrams, samples show both tholeiitic (THI > 1) and calc-alkaline affinity (THI < 1), with values between 0.8 and 1.1.

Harker bivariate plots show a fairly defined positive correlation of SiO_2 with Na_2O, and clear negative correlations with CaO, MgO, and

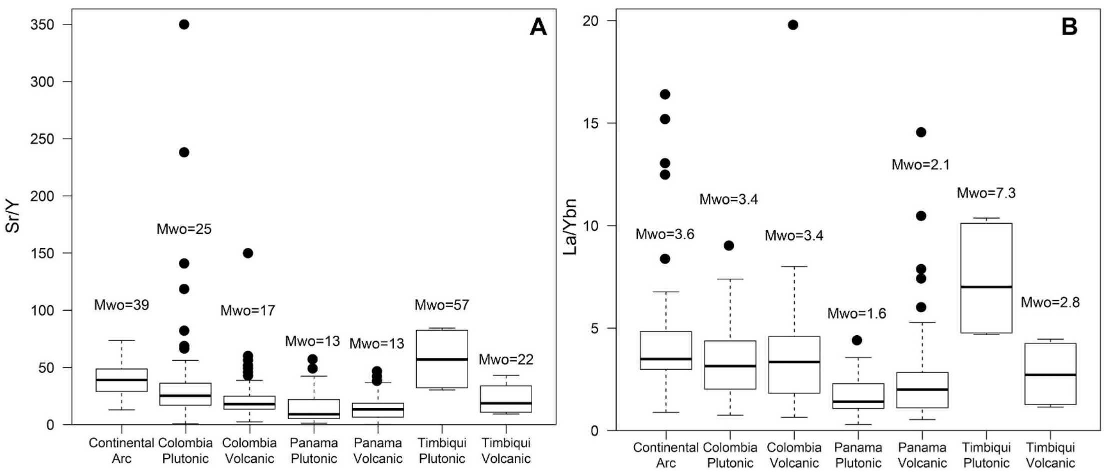

Fig. 4. Boxplots showing the distribution of A) Sr/Y ratios and B) La/Yb$_N$ values (after Nakamura, 1974) for each geological domain presented in text. Mwo = mean value after removing outliers (represented by black dots).

Fe_2O_3 total, which may reflect magmatic differentiation (Fig. 6A). Multi-elemental diagrams normalized to N-MORB (Sun and McDonough, 1989), show a variable enrichment in the LILE including Th and Ce, and a common well-defined negative Nb and Ti anomalies (Fig. 5C). The REE patterns show weak to strong enrichment in LREE, whereas HREE are characterized by a flat trend (Fig. 5D). Mean Sr/Y values of 13 were estimated for both the Panamanian plutonic and volcanic rocks (Fig. 4A). Plutonic rocks yielded a mean $(La/Yb)_N$ ratio of 1.6, whereas the volcanic units yielded a mean $(La/Yb)_N$ value of 2.1 (Fig. 4B).

Published Sr-Nd-Pb whole-rock isotopes, and new analyses conducted in this work, are characterized by depleted mantle values, with $^{87}Sr/^{86}Sr_{(i)}$ varying between 0.7027 and 0.7044, and $\varepsilon Nd_{(i)}$ values between 5.3 and 8.2. The $^{206}Pb/^{204}Pb$ ranges from 18.643 and 19.152,

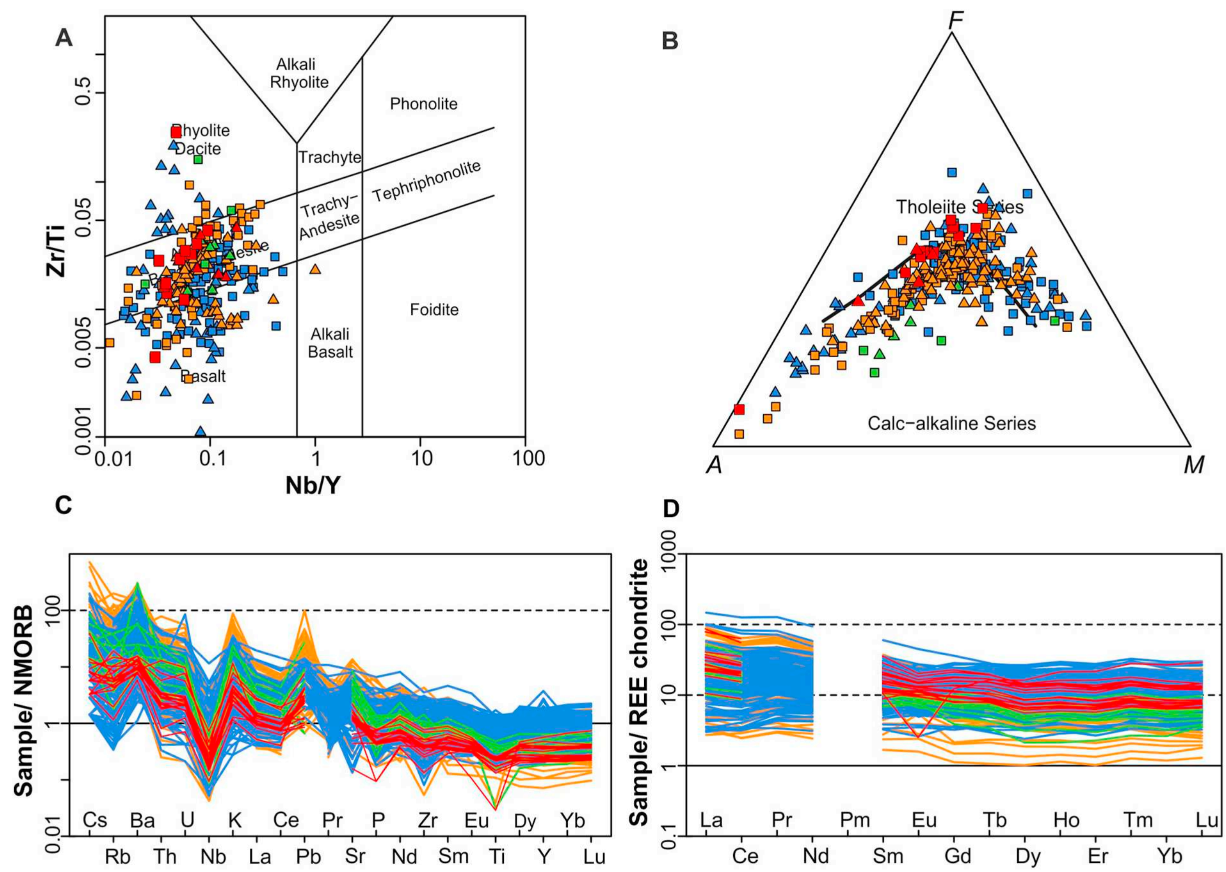

Fig. 5. Classification and spider diagrams of Paleocene – Eocene arc-related Panamanian and Colombian rocks. A) Nb/Y vs Zr/Ti classification diagram after Winchester and Floyd (1977; modified after Pearce, 1996); B) AFM diagram after Irvine and Baragar (1971); C) Multi-elemental diagram normalized to NMORB after Sun and McDonough (1989); D) REE spider diagram normalized after chondrite values of Nakamura (1974). Squares and triangles are for plutonic and volcanic samples, respectively. In blue Panamanian units; orange Colombian units; in red new results presented in this work from the Santa Cecilia-La Equis and the Acandi Batholith; green samples from Timbiqui Complex and associated intrusives. (For interpretation of the references to color in this figure legend, the reader is referred to the web version of this article.)

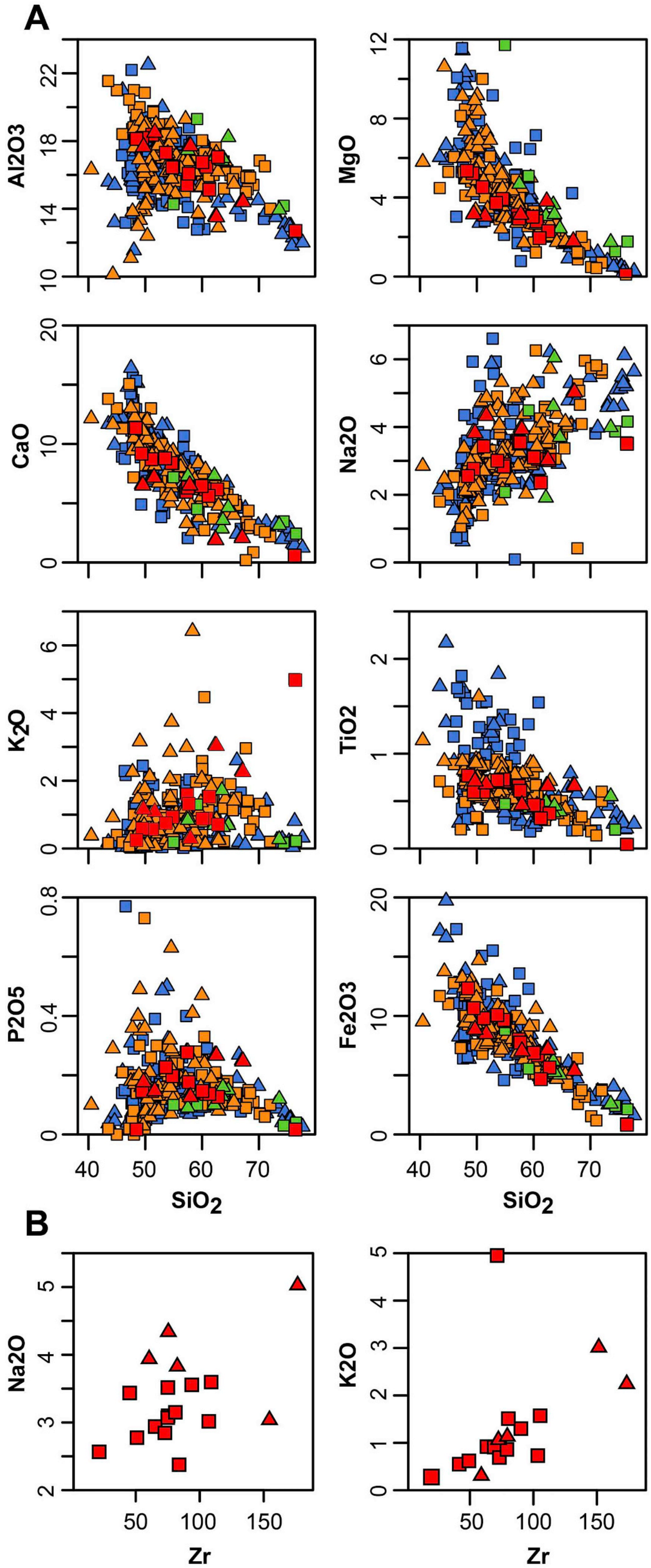

Fig. 6. A) Harker bivariate diagrams showing the relation of major oxides for samples from the Paleogene Panama Arc and Timbiqui Complex arc-related rocks. B) Bivariate diagrams Zr vs. Na_2O and K_2O for samples analyzed in this study. Same symbology of Fig. 4.

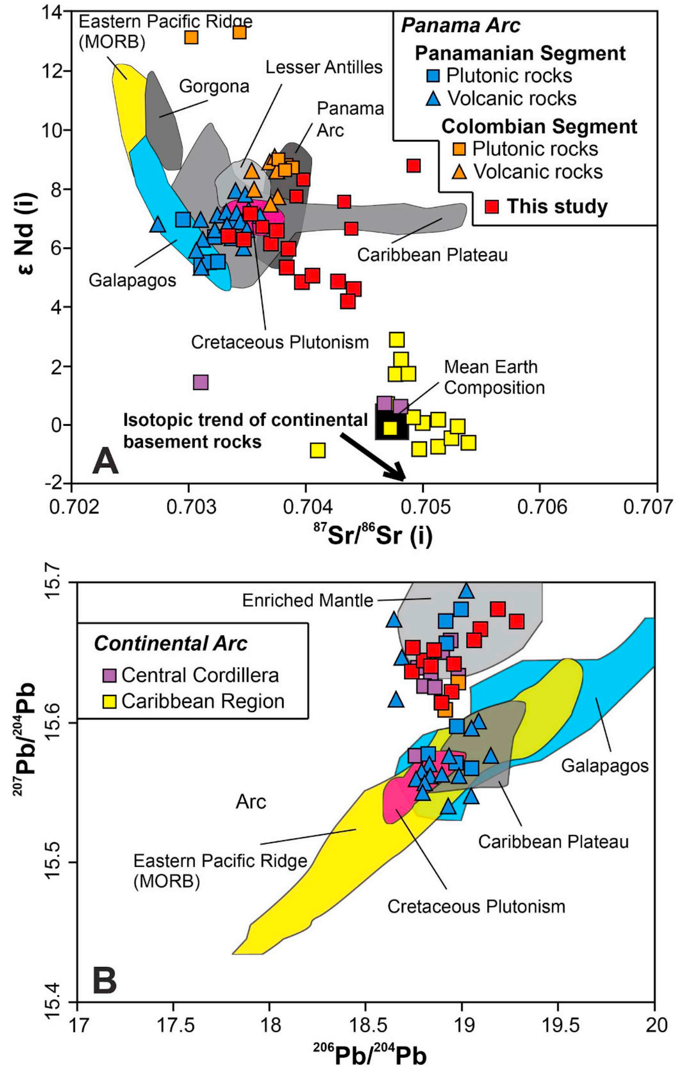

Fig. 7. $^{87}Sr/^{86}Sr_{(i)}$ vs. $\varepsilon Nd_{(i)}$ and $^{206}Pb/^{204}Pb$ vs. $^{207}Pb/^{204}Pb$ diagrams (after Thompson et al., 2004 and references therein) for both continental and oceanic Paleocene – Eocene arc-related units presented in text. Same symbology of Figs. 2 and 5.

$^{207}Pb/^{204}Pb$ from 15.539 to 15.697 and $^{208}Pb/^{204}$ Pb varies between 38.418 and 38.88 (Fig. 7). Such values are akin to oceanic arcs, which are characterized by a prominent mantle input lacking of older radiogenic basement. Furthermore, the variations of Pb isotopic values suggest additional input from an enriched mantle. It is noteworthy that the isotopic signature of the plutonic rocks, although similar to that of the volcanic units, present slightly higher $^{87}Sr/^{86}Sr_{(i)}$ values.

4.2.2. Colombian volcanic and plutonic rocks

Volcanic and plutonic rocks Paleogene in age, which have been correlated with the Panama Arc, are included in the Santa Cecilia-La Equis Complex, and the Acandi and Mande batholiths (Gonzalez, 2001). These units crop out along the western flank of the Western Cordillera and in the northwestern Urabá Region of Colombia, and represent the eastward and southeastward extension of the San Blas and Darien Ranges in Panama. The volcanic rocks from the Santa Cecilia-La Equis complex include basaltic to andesitic lava flows, as well as porphyritic intermediate units, with minor pyroclastic rocks (this contribution, Buchely et al., 2009; Rodríguez et al., 2010; Salazar et al., 2005). Intermediate units (i.e., gabbro-diorite-tonalite) dominantly represent the plutonic rocks from the Acandi and Mande batholiths, with granodiorite, monzodiorite and granites present in minor proportion

(González and Londoño, 2002; Rodríguez et al., 2010; Salazar et al., 2005). The intermediate-acid plutonic rocks of the Acandi and Mande batholiths, intrude basic-intermediate volcanic rocks from the Santa Cecilia-La Equis Complex (Calle and Salazar, 2007; González and Londoño, 2002).

Available zircon U-Pb crystallization ages for these rocks span between ~59 Ma and ~42 Ma, with additional K/Ar and Ar/Ar ages, which may reflect either crystallization or cooling ages ranging from ~55 Ma to ~34 Ma (see Supplementary material Table S2 for references). However, the aforementioned paucity of geochronological data for the Panama Arc-related Colombian rocks hinders the discrimination of different magmatic episodes, as those older than 60 Ma registered in the Panamanian units. Middle to late Eocene pyroclastic rocks as well as siliciclastic coarse-grained deposits with both volcanic and plutonic lithic fragments on top of the main volcanic sequence of the Santa Cecilia-La Equis, are interpreted as the subaerial and erosional expressions of the Panama Arc (León et al., 2018; Montes et al., 2012a; Rodríguez and Sierra, 2010).

Five analyzed samples from the Santa Cecilia-La Equis Complex, are mainly represented by silicified and hydrothermally altered porphyritic basalts and andesites and minor pillow-lava intermediate in composition. Since most of the samples show significant alteration, we rather used relatively immobile elements such as Nb, Ti, Zr, and Yb (Pearce, 1996), in order to classify them appropriately (Fig. 5A). SiO_2 values vary from 49.4 wt% to 67 wt% in the most silicified samples, and total alkalis ranges between 4.3 wt% and 7.4 wt%, whereas Fe2O3 and MgO span from 5.48 wt% to 8.9 wt%, and 1.82 wt% to 3.8 wt%, respectively. In the AFM diagram, samples follow both tholeiitic and calc-alkaline trends (Fig. 5B). Harker bivariate diagrams, show fairly defined negative correlations of SiO_2 with Al_2O_3, Fe_2O_3 and CaO, which may be related with magmatic differentiation, whereas the cloudy pattern of K2O and Na2O (Fig. 6A) suggest elemental mobility and alteration, as also indicated by the lack of a linear trend when plotted against Zr (Fig. 6B). Multi-elemental patterns normalized to NMORB (Sun and McDonough, 1989) are characterized by a slight enrichment in the LILE such as Cs, Rb and Ba, with well-defined negative anomalies of Nb and Ti (Fig. 5C). REE normalized to the chondrite values (Nakamura, 1974) show a relative steep pattern (Fig. 5D), as suggested by the $(La/Yb)_N$ ratio varying from 4.2 to 6.0.

Thirteen analyzed samples from the Acandi Batholith mostly include variably altered intermediate and minor acidic rocks. Alike the samples from the Santa Cecilia-La Equis, we evaluate the compositional features of this unit by using the abundances of elements such as Nb, Ti, Yb, Zr, which are considered immobile during hydrothermal processes (Fig. 5A; Pearce, 1996). SiO_2 varies between 48.1 wt% and 76.3 wt%, with total alkalis ranging from 2.9 wt% and 8.6 wt%, whereas Fe_2O_3 and MgO range from 0.9 wt% to 12.4 wt%, and 0.1 wt% to 5.4 wt%, respectively. Analyzed samples follow both tholeiitic and calc-alkaline trends in the AFM classification diagram (Fig. 5B). Alike the Panamanian rocks, the plutonic and volcanic rocks from the Colombian segment analyzed here (Santa Cecilia Complex and Acandi Batholith), also show a bimodal tholeiitic and calc-alkaline affinity in the Zr/Y and Th/Yb diagram (see Fig. S1; Ross and Bédard, 2009). Harker bivariate diagrams show well-defined negative correlations of SiO_2 and Fe_2O_3, CaO and MgO (Fig. 6A), which may represent magmatic differentiation, whereas cloudy patterns of K_2O, Na_2O and Al_2O_3 indicate elemental mobility and alteration, supported by the absence of a linear trend when compared against Zr (Fig. 6B). As observed in the volcanic samples from the Santa Cecilia-La Equis Complex, the multi-elemental patterns normalized to NMORB of rocks from the Acandi Batholith, show a slight enrichment in the LILE with strongly defined negative anomalies of Nb and Ti (Fig. 5C). REE abundances normalized to the chondrite values (Nakamura, 1974) show both flat to steep patterns as suggested by the (La/Yb)N ratio spanning between 0.9 and 5.3 (Fig. 5D). One sample present a strong Eu negative anomaly (Eu/Eu* = 0.2), which may indicate plagioclase fractionation in the magmatic system.

Previously published geochemical data show that the Santa Cecilia-La Equis Complex and the Acandi and Mandé batholiths are mostly intermediate in composition, including mainly basaltic-andesites and its plutonic equivalents, with minor basic and acid rocks (Fig. 5A). In the AFM and Zr/Y vs. Th/Yb diagrams, samples dominantly plot within both the calc-alkaline and tholeiitic fields (Fig. 5B, see also Fig. S1). Harker bivariate diagrams show weak positive correlations of SiO_2 with Na_2O, whereas well-defined negative correlations with CaO, MgO, and Fe_2O_3 are observed, which may be related to fractional crystallization of the major mineral phases such as feldspar, pyroxene and amphibole (Fig. 6A). Multi-elemental patterns, normalized to the N-MORB composition of Sun and McDonough (1989), are similar to the Panamanian segment, with enrichment in LILE such as Th and Ce, together with weak to strong Nb and Ti negative anomalies (Fig. 5C). REE abundances show moderate enrichment in the LREE with flat HREE (Fig. 5D). The Colombian plutonic and volcanic rocks related to the Panama Arc show mean Sr/Y values of 25 and 17, respectively (Fig. 4A). As for the Panamanian units, those values are considerably lower than those estimated for continental-affinity rocks. Furthermore, plutonic and volcanic rocks from the Colombian segment yielded a similar mean $(La/Yb)_N$ ratio ca. 3.4 (Fig. 4B).

Since no isotopic data from the volcanic rocks of the Panama Arc in the Colombian segment are available so far, we focus our discussion in the Sr-Nd-Pb-Hf isotopes of the plutonic rocks.

New Sr-Nd results obtained from the Acandi Batholith, and published data from the Mande Batholith (Sánchez-Celis et al., 2018; Leal-Mejía, 2011), are characterized by juvenile values with $^{87}Sr/^{86}Sr_{(i)}$ varying between 0.7032 and 0.7050. $^{143}Nd/^{144}Nd_{(i)}$ ranges between 0.512901 and 0.513275 with $\varepsilon Nd_{(i)}$ between 6.4 and 13.6. Pb isotopic signature of the same samples is characterized by $^{206}Pb/^{204}Pb$ values between 18.758 and 18.969, $^{207}Pb/^{204}Pb$ ranging from 15.610 to 15.643, and $^{208}Pb/^{204}Pb$ spanning between 38.560 and 38.704 (Fig. 7). Such results are similar to those described above for the Panamanian volcanic and plutonic rocks.

Twenty zircon crystals from one sample of the Acandi Batholith (sample GA-003) were analyzed for Hf isotopes. The initial $^{176}Hf/^{177}Hf_{(i)}$ ratio varies between 0.283060 and 0.283129 which are depicted by $\varepsilon Hf_{(i)}$ values from 10.8 to 13.2, which suggest a juvenile mantle source close to the depleted mantle fingerprint (Fig. 8). Although the new reported Hf isotopes are similar to those recorded in some of the Panamanian plutons (Ramírez et al., 2016), these authors also found lower $\varepsilon Hf_{(i)}$, which may reflect oceanic sediment contribution to the magmatic sources (Vervoort et al., 1999; Chauvel et al., 2008).

4.3. Timbiqui Complex

In the western foothills of the Western Cordillera and the Pacific region of southwestern Colombia, a volcano-sedimentary succession intruded by a series of small intermediate plutonic and sub-volcanic bodies, crops out (ANH-GRP, 2011, ANH-Universidad de Caldas, 2011; Annells et al., 1988; McCourt et al., 1990a, 1990b). This magmatic domain includes andesitic lavas and tuffs, agglomerates and breccia, overlain by fossiliferous mudstones and sandstones, which are separated to the east from the Cretaceous volcano-sedimentary units of the Western Cordillera by the prominent N to NNE trending regional Junín-Sambiambí Fault (Gómez-Tapias et al., 2015).

The Timbiqui Complex is also reported in fault contact with a series of highly deformed gabbros and serpentized peridotites from the Guapi Ultramafic Complex, which are intruded by deformed tonalitic and andesitic dikes with a zircon U-Pb age of 53.3 ± 0.3 Ma (ANH-GRP, 2011). Minor basic to intermediate plutonic units, including gabbros, diorites, and tonalites (i.e., Rio Napi Intrusive, Balsitas Pluton, and El Salto Pluton), have been associated to the Timbiqui Complex (McCourt et al., 1990a, 1990b).

Upper Eocene to Oligocene sequences of external platform environments overly the Timbiquí Complex and its basaltic Cretaceous

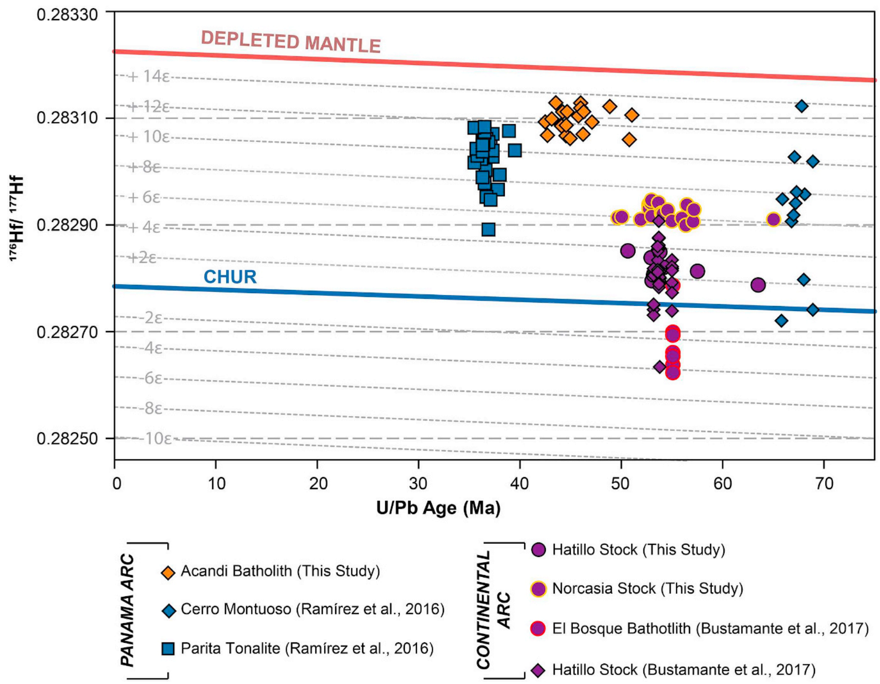

Fig. 8. Hf isotope data for samples analyzed in this study and compiled from Bustamante et al. (2017) and Ramírez et al. (2016), for both the Panama and the continental arcs.

basement (ANH-GRP, 2011; ANH-Universidad de Caldas, 2011; Borrero et al., 2012; Echeverri et al., 2015a; López-Ramos, 2009). Miocene – Pliocene sandy and conglomeratic siliciclastic sediments of the Raposo and Mayorquín formations overly these units in angular unconformity (ANH-GRP, 2011; ANH-Universidad de Caldas, 2011; Annells et al., 1988).

K/Ar ages between ~53 Ma and ~32 Ma have been reported for different andesitic lavas, porphyries, and tuffs, as well as for the associated basic-intermediate plutonic bodies (McCourt et al., 1990a, 1990b). Although these ages may be meaningful, the nature of the analyzed material is not described; therefore no further interpretations can be done regarding the geological meaning of them. However, a zircon U-Pb analysis conducted on andesitic lava, suggest a crystallization age of 44.2 ± 0.5 Ma (ANH-GRP, 2011), confirming an Eocene age for this magmatism.

Geochemically, rocks from the Timbiqui Complex and associated plutonic rocks (i.e., Middle Eocene Magmatic Event; ANH-GRP, 2011), are dominantly intermediate in composition, including andesites, tonalites, and quartzdiorites, which follow a calc-alkaline magmatic trend (Fig. 5A, B). Harker bivariate plots show slightly to strongly defined negative correlations between SiO_2 and CaO, MgO, Fe_2O_3 and Al_2O_3, and a poorly defined positive correlation with Na_2O, which may suggest the existence of fractional crystallization processes (Fig. 6A). Multi-elemental patterns normalized to NMORB after Sun and McDonough (1989) exhibit enrichment in the LILE such as Cs, Rb, Ba, and Th, with strong to weak negative anomalies of Nb and Ti (Fig. 5C). REE abundances when normalized to the chondrite composition of Nakamura (1974) show a notable enrichment in the LREE, whereas the MREE and HREE present a flat pattern (Fig. 5D).

When analyzing the mean Sr/Y and $(La/Yb)_N$ values of the Timbiqui Complex rocks and associated plutons an outstanding feature is observed. Intermediate plutonic rocks (i.e., Middle Eocene Magmatic Event, ANH-GRP, 2011) show a mean Sr/Y ratio of 57, whereas the andesite and andesitic tuffs present a mean Sr/Y value of 22 (Fig. 4A). Moreover, plutonic and volcanic units yielded a mean $(La/Yb)_N$ value of 7.3 and 2.8, respectively (Fig. 4B).

Coeval magmatic units have been described in the Western Cordillera of Ecuador (i.e. Macuchi Arc; Vallejo et al., 2009), which include basaltic to dacitic effusive and pyroclastic rocks showing both MORB-like and IAT-like geochemical affinities (e.g. Hughes and Pilatasig, 2002; Lebras et al., 1987). Available Ar/Ar and U-Pb zircon radiometric ages for the volcanics range from ~42 to 35 Ma (Vallejo et al., 2009), and detrital zircon U-Pb analyses in associated sediments have shown the presence of Permian-Triassic and older ages (Vallejo et al., 2009). This Paleocene-Eocene arc-related rocks was initially considered as an accreted island arc intruding Cretaceous oceanic crust, however the older host rocks was apparently already accreted to the continent in the Paleogene and together with presence of older detrital zircons have been used to suggest that it represent a Paleogene continental arc (Chiaradia, 2009; Vallejo et al., 2009).

5. Discussion

We presented a review of published and new temporal and compositional constraints of the early Paleocene to middle Eocene magmatic rocks exposed in the Colombian Andes and central – eastern Panama, which allowed us to characterize not only the shared arc-related geochemical signature (Fig. 9), but also their chemical and isotopic particularities. Although it has been demonstrated that at least two different tectono-magmatic domains exist, including a continental and a dominantly oceanic island arc, they together reflect the complex tectonic interactions between the South American, Caribbean and Farallon plates during the Paleogene. In this section, we evaluate causal relationships between the regional-scale kinematic framework and the magmatic record described above in order to better explore its tectonic implications. See Fig. 11 for a plausible paleogeographic snapshot at for the early – middle Eocene of the northwestern margin of South America and the southwestern Caribbean.

5.1. Paleogene transition from collision to oblique subduction and the magmatic record of the continental margin

Plutonic rocks exposed in the Central Cordillera and northeastern Caribbean region of Colombia (Santa Marta and Guajira), formed after the Late Cretaceous arc-continent collision of the South-American margin with the leading edge of the Caribbean Plate (Bustamante et al.,

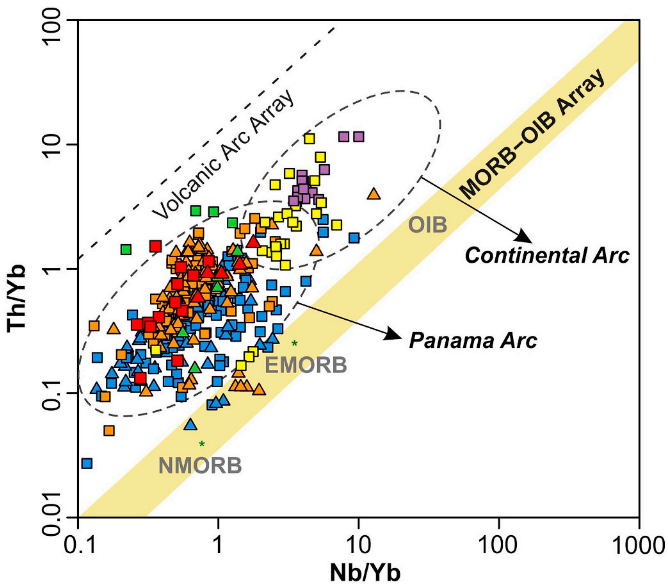

Fig. 9. Tectonic discrimination diagram of discussed Paleocene – Eocene magmatic units from compiled and new geochemical data, after Pearce (2008). Same symbology of Figs. 2 and 5.

2017; Cardona et al., 2011a, 2011b; Pindell et al., 2005; Villagómez et al., 2011). This oceanic plate was formed during the Cretaceous (> 90 Ma) as a large igneous province in southwestern Pacific latitudes, until it achieved its inter-American position since the Late Cretaceous (Burke, 1988; Lugo and Mann, 1995; Pindell and Barret, 1990; Pindell and Kennan, 2009; Hincapié-Gómez et al., 2018). Geophysical constraints have revealed that the Caribbean plate thickness varies from typical oceanic crust values of ca. 5–10 km to values as high as 18 km (Case et al., 1990; Mauffret and Leroy, 1997; Diebold and Driscoll, 1999). It has been commonly argued, based on buoyancy analyses that oceanic plateaus are normally hard to subduct (Closs, 1993; Whattam and Stern, 2015). However, more recent numerical and analogue models have shown that oceanic plateaus can subduct when they are characterized by an homogeneous crust, lacking of a basal detachment or when they are immerse into an older lithosphere (Tetreault and Buiter, 2012; Vogt and Gerya, 2014). Additionally, when the lower crust of oceanic plateaus reach medium- to high-grade metamorphism their bulk density significantly increase prompting subduction at convergent margins (Closs, 1993).

It is therefore arguable that an heterogeneous Caribbean oceanic plate was able to subduct underneath northwestern South America, resulting in the construction of a continental magmatic arc (Bayona et al., 2012; Bustamante et al., 2017; Cardona et al., 2011a, 2011b, 2014), as seen in similar geodynamic settings (Timm et al., 2014). Remnants of a metamorphosed Caribbean plateau lower crust found in Ecuador (Beaudon et al., 2005) and Colombia (Correa et al., 2017; Rodriguez et al., 2012), may suggest that associated changes in density and buoyancy facilitated its sinking into the sub-continental mantle.

The resulting continental arc was a short-lived magmatic episode (U-Pb ages between ~60–45 Ma) characterized by a well-defined convergent-margin geochemical signature, with some plutonic bodies with steep REE patterns, high Sr/Y ratios and variable Y content (Fig. 10). Such REEs pattern can be related to high-pressure melting/differentiation in the garnet stability field in a relatively thickened crust, which is consistent with an inherited crustal structure that resulted from the Late Cretaceous-Paleocene orogenic phases (Bustamante et al., 2017). A mean crustal thickness of ~51 km for the continental arc system, was estimated from the Sr/Y data of Bustamante et al. (2017), following Chapman et al. (2015) methodological approach. High Al_2O_3 and Na_2O values, suggest that mafic crust melting may have occurred associated to the high heat-flow during the early stages of subduction of the Caribbean plate (Cardona et al., 2011a, 2011b, 2014). Other plutons instead present a more flat REE trend and have lower Sr/Y values (Fig. 10), which has been interpreted as the result of along-strike differences in crustal thickness (Bustamante et al., 2017). Whole-rock Sr-Nd-Pb as well as the zircon Hf isotopic record are characterized by a mixture of both juvenile and radiogenic values (this contribution; Bustamante et al., 2017; Cardona et al., 2011a, 2011b, 2014; Leal-Mejía, 2011), which is likely to be related to a mixture between older continental crust and mantle or cretaceous basaltic crust in the magma sources.

The along-strike variations in crustal thickness, and the elongated nature of the Paleocene-Eocene plutons of the Central Cordillera, suggest a structural control during the emplacement of the magmatic rocks, probably triggered by oblique convergence between the Caribbean and South-American plates. Magnetic anisotropy analyses conducted in the Santa Marta Batholith suggest a major tectonic control during its

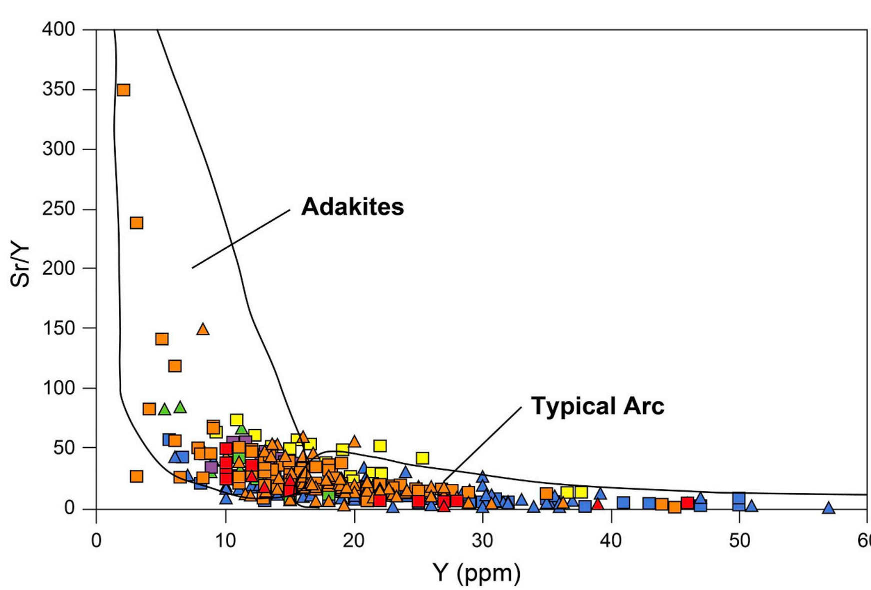

Fig. 10. Y vs. Sr/Y diagram showing the typical arc signature of most of the samples included in this work, as well as the adakite-like affinity of some rocks from the Panama, Timbiqui and Continental arcs.

emplacement (Salazar et al., 2016). The syn- and post-magmatic transpressional-transtensional tectonics is thought to represent a tectonic scenario that shaped the margin throughout most of the Cenozoic (review in Montes et al., 2010; Pindell and Kennan, 2009; Zapata et al., 2014). This geodynamic setting is also responsible for the fragmentation of the Paleocene – Eocene Arc and the translations of some of its remnants to the northeastern Caribbean Region of Colombia (Cardona et al., 2014).

Middle Eocene volcanic material has been recognized east of the Central Cordillera within Paleogene foreland basins, as far as 400 km inland from the main magmatic front, which may reflect transient flattening of the subduction angle (Bayona et al., 2012). Syn-collisional Paleocene depocenters, exposed in eastern Colombia (Magdalena Valley), were uplifted as a series of discontinuous blocks, which has been attributed to the re-activation of older extensional structures (Bayona et al., 2012), probably under a partitioned strain regime, triggered by oblique convergence that resulted in differential along-strike deformation and exhumation (Parra et al., 2009).

Post-middle Eocene magmatic quiescence has been related to strongly oblique convergence and the flat subduction of the thick plateau-like Caribbean crust (Bayona et al., 2012; Bustamante et al., 2017; Cardona et al., 2011a, 2011b), until it resumed in the Late Oligocene-Miocene with the built of the Cenozoic Andean arc as consequence of the subduction of the Nazca plate (Aspden et al., 1987).

5.2. Paleocene – Eocene island arc magmatism and its geodynamic and paleogeographic implications

The arc-related rocks from Panama, the Uraba Region and the Western Cordillera of Colombia present strikingly similar geochronological, geochemical and isotopic characteristics, which together with their structural position, suggest that they are part of a common magmatic domain as previously suggested by Duque-Caro (1990).

Arc-like magmatism in Panama has been thought to initiate at ca. 71 Ma (Buchs et al., 2010), extending until the Oligocene when a period of quiescence interrupted the protracted magmatic history, re-starting at ca. 25 Ma (Rooney et al., 2010; Wegner et al., 2011). Although more data is still necessary, the presence of ~68–66 Ma calc-alkaline plutons and dacites, suggest that arc magmatism in Panama must have initiated earlier than 70 Ma as previously considered, since the switch from early-subduction forearc MORB-like magmatism to a well-established typical arc system may take ca. 10 m.y. (Ishizuka et al., 2014; Whattam and Stern, 2011). It is therefore expected that subduction initiation may have occurred earlier than the Maastrichtian, as suggested by: 1) the presence of volcano-clastic sandstones in Coniacian units from the Nicoya Complex in Costa Rica (Pindell and Kennan, 2009), and the re-interpretation of the forearc basaltic sequences of Panama and Costa Rica as associated to subduction initiation (Whattam and Stern, 2015). In Colombia U-Pb geochronological constraints have shown that the magmatic record may extend between ~59 and 34 Ma, with more geological and geochronological constraints still necessary in order to track the older arc-related products.

The detrital U-Pb record of middle Eocene and younger sedimentary sequences in Panama (i.e. Gatuncillo, Cobachón, Tonosí, Cucaracha, Culebra formations; Montes et al., 2012a, 2012b; Ramírez et al., 2016), including modern river sediments, are characterized by a major cluster of individual ages between ~60 Ma and ~40 Ma, with minor Late Cretaceous, Oligocene and younger zircons. This feature, when combined with the analysis of the temporal distribution of the compiled Ar-Ar, K-Ar and U-Pb ages, suggest the existence of a ca. 40–50 Ma magmatic flare-up (Fig. 12A). We speculate that this major phase of magmatic activity may have been triggered by a change towards a faster and strongly orthogonal subduction of the Farallon Plate beneath the trailing edge of the Caribbean plate, where the Panama Arc was constructed. This probable geodynamic configuration, which has been kinematically restored in global plate tectonic reconstructions (Seton et al., 2012), favors strong slab dehydration that may increase melt volumes generated from the subduction-modified mantle (Davies and Bickle, 1991; George et al., 2003; Zellmer, 2008). The LILE and LREE enrichment of plutonic and volcanic rocks described above, indicate that slab-derived fluid assisted melting, together with arc thickening, was taking place during the middle Eocene. The increased generation of subduction-related magmas and the changes in convergence vectors in the Pacific are likely to be linked with the collision of the leading edge of the Caribbean plate (Greater Antillean Arc; review in Pindell et al., 2012) with North America that took place during the Eocene (Iturralde-Vinent et al., 2016) and cause the Caribbean plate to slow down its northeastern displacement (Fig. 12B).

It is also plausible that arrival of thick and buoyant Caribbean oceanic plate beneath the north-Andean margin may hampered its northeastward displacement until the Late Eocene (Fig. 12B; Pindell and Kennan, 2009). The subsequent plate motion acceleration and its ongoing eastward migration is recorded in the evolution of the Cayman Ridge, and the complex basin-opening and along-strike block translations in the northern Caribbean margin of South America (review in Pindell and Kennan, 2009; Zapata et al., 2014).

As for the continental Paleogene arc, we estimated a possible depth of magma generation by using the Sr/Y ratios obtained from the compiled geochemical database of Panama Arc-related rocks (Fig. 10). Our results suggest that the mean crustal thickness of the Panama Arc during the generation of the above-described units, oscillates between 15 km to 30 km, which reflect inherited variations in the plateau-like oceanic crust where the magmatic rocks were formed and the local increase on arc crustal thickness due to magmatic underplating.

5.3. Plausible tectonic scenarios for the origin of arc-related rocks from the Timbiqui Complex

The significance of the Timbiqui Complex arc system within the paleogeographic framework of the northern Andes remains poorly understood. Nevertheless, two different models have been proposed from regional considerations. A first model indicates a para-autochthonous origin associated to the continental South-American margin (Pindell and Kennan, 2009). Conversely, Echeverri et al. (2015a) argued that the modern > 100 km distance between the Timbiqui and the Central Cordillera arc related segments, together with their characteristic arc-front-related geochemistry and the absence of a typical high-K and enriched signature of a distal rear-arc (Tatsumi and Eggins, 1995), suggest that both domains could not represent a single arc system. Therefore, the Timbiqui rocks must represent an exotic terrane.

Overlying siliciclastic sedimentary sequences of late Eocene to Miocene in age, record the final assembling of this domain to the southwestern Colombian margin (Echeverri et al., 2015a, 2015b, 2016). A similar discussion has been presented for the Paleogene Macuchi Arc in the Western Cordillera of Ecuador (Hughes and Pilatasig, 2002; Vallejo et al., 2009). The Macuchi Arc however is interpreted as a continental arc, with an oceanic arc-related composition considered as an inherited fingerprint of their host rocks related to Cretaceous accreted basaltic terranes. Consequently, it is interpreted as an autochthonous magmatic arc generated in the continental Ecuadorian margin, as is also supported by the presence of continent-derived detritus in associated sedimentary units (e.g. Angamarca Group; Pindell and Kennan, 2009; Vallejo et al., 2009).

Available geochemical data from the volcanic rocks of the Timbiqui Complex, show moderately-steep REE patterns (mean $(La/Yb)_N$ ratio of 2.76), which are characteristic of a moderately mature arc formed in a mid-shallow melting environment (Profeta et al., 2015 and references therein), as indicated by the mean crustal thickness of ~20 km estimated from the Sr/Y ratio. In contrast, the geochemical behavior of the intermediate-felsic plutons associated to this arc (i.e. Middle Eocene Magmatic Event; ANH-GRP, 2011), is however puzzling. High Sr/Y and $(La/Yb)_N$ values of 57 and 7.3, respectively, SiO_2 > 56 wt%, and

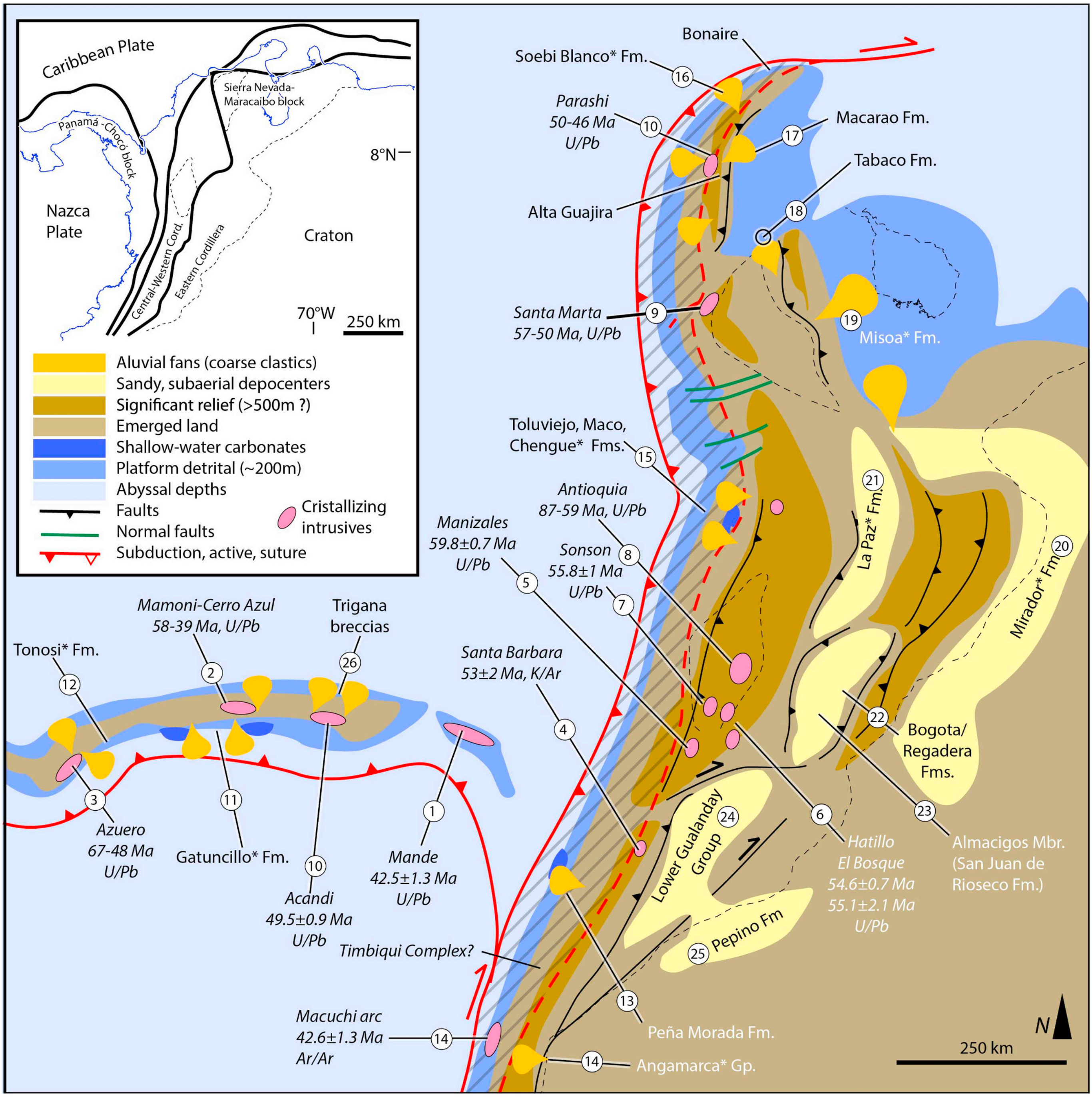

Fig. 11. Palinspastic paleogeographic reconstruction of the northern Andes and southern Caribbean for Eocene to early Oligocene times (~50 to 30 Ma). Modified from Cardona et al. (2014), Reyes-Harker et al. (2015), and Rodriguez-Parra et al. (2017). Diagonal pattern shows accreted plateau and arc fragments (Kerr et al., 2003). Crystallizing/cooling plutonic bodies during this time interval: 1: Mande batholith (Villagómez et al., 2011; Montes et al., 2012b; Montes et al., 2015); 2: Mamoni-Cerro Azul intrusive suite (Wegner et al., 2011; Montes et al., 2012b); 3: Azuero intrusives (Wegner et al., 2011; Montes et al., 2012a; Ramírez et al., 2016); 4: Santa Barbara batholith (cooling age, McCourt et al., 1984); 5: Manizales stock (Bayona et al., 2012); 6: Hatillo stock (Bayona et al., 2012; Bustamante et al., 2017); 7: Sonson batholith (Leal-Mejía, 2011; Ordoñez-Carmona et al., 2011); 8: Antioquia batholith (Leal-Mejía, 2011; Bayona et al., 2012); 9: Santa Marta batholith and Parashi stock (Cardona et al., 2011a, 2011b); 10: Acandi batholith (Montes et al., 2015); 14: Macuchi arc (Vallejo et al., 2009). Early to middle Eocene strata, asterisk where corresponding Paleocene-middle Eocene U/Pb detrital zircon ages are available: 11: Gatuncillo Formation (Woodring, 1964; Ramírez et al., 2016); 12: Tonosi Formation (Del Giudice and Recchi, 1969; Kolarsky et al., 1995; Krawinkel et al., 1999; Herrera et al., 2012; Ramírez et al., 2016); 13: Peña Morada Formation (Borrero et al., 2012); 14: Angamarca Group (Vallejo et al., 2009); 15: Toluviejo, Maco and Chengue Fms. (Flinch, 2003; Rincón et al., 2007; Cardona et al., 2012); 16: Soebi Blanco Formation (Priem et al., 1986; Zapata et al., 2014); 17: Macarao Formation (Rollins, 1965); 18: Tabaco Formation (Montes et al., 2010; Bayona et al., 2011); 19: Misoa Formation (Escalona and Mann, 2006; Escalona and Mann, 2011; Xie et al., 2010); 20: Mirador Formation (Mora et al., 2010); 21: La Paz Formation (Nie et al., 2010); 22: Bogota Formation (Moron et al., 2013); 23: Almacigos Member of the San Juan de Rio Seco Formation (Gómez et al., 2003); 24: Lower Gualanday Group (Anderson, 1972; Caicedo and Roncancio, 1994); 25: Pepino Formation (Borrero et al., 2012); 26: Trigana and Tripogadi informal units (Rodríguez and Sierra, 2010).

Yb < 1.3 ppm suggest an adakite-like geochemical signature and thicker crust (Fig. 10), also reported farther to the south in the volcanic and plutonic rocks of the Macuchi Arc (Chiaradia, 2009), which is interpreted as a fingerprint of the plateau-like basement melting on deep and thick crustal environment.

Although more data is still necessary to evaluate the plausible paleogeographic implications of this magmatic arc, we suggest that during the Paleogene, the Timbiqui Complex was allochthonous to the Colombian continental margin, but may still be considered as para-autochthonous to the continental margin. This arc may represent either a tectonically dismembered segment or an oceanic continuation of the Ecuadorian Macuchi arc, similar to what is seen in the Aleutians, where the magmatic arc in the Alaska Peninsula is of continental affinity but it laterally changes to an oceanic arc southwestward (Yogodzinski et al., 2010). Pindell and Kennan (2009) have suggested that during the Late Paleocene-Early Eocene (see their reconstruction at 56 Ma), the trailing edge of the Caribbean plate, in which the Central American arc was growing, collided with the Ecuadorian margin. Therefore, during the Eocene the continental-transitional Macuchi and Timbiqui arc-related rocks were likely continuous with the oceanic Panama Arc (Figs. 11 and 12). The final juxtaposition and disruption of this arc along the Andean margin may have resulted from the progressive zipper-like collision of Panama with Colombia and the Cenozoic oblique subduction of the Nazca plate that favors tectonic scape (Mann and Corrigan, 1990; Pindell and Kennan, 2009).

6. Conclusions

In the Colombian and Ecuadorian Andes, as well as in the Darien, San Blas and Azuero regions of Panama, a discontinuous series of Paleogene volcanic and plutonic rocks crop out, which intrude both Cretaceous oceanic plateau-like crust and the older continental basement of northwestern South America. The Paleocene – Eocene (~60–45 Ma) stock and batholith-sized units that intrude the pre-Cretaceous basement of the Central Cordillera and the northeastern Caribbean region of Colombia, represent the short-lived magmatic record of the Caribbean plate subduction underneath the previously thickened continental crust. This domain is characterized by the enrichment in incompatible elements, strong Nb and Ti negative anomalies and the high Sr/Y ratios, together with a Sr-Nd-Pb-Hf mixed radiogenic and mantle isotopic signature that indicate a heterogeneous magma source, which is expected for an arc system constructed on a thickened continental margin where oceanic terranes were accreted before. The coeval volcanic and plutonic rocks of western Colombia and Panama included within the Panama Arc, also exhibit an arc-related geochemical signature such as the enrichment in LILE, steep LREE patterns and Nb-Ti negative anomalies. However, Sr-Nd, as well as Pb isotopes of this domain, are akin to juvenile magma sources and do not reflect any clear contribution of radiogenic material, although previous stratigraphic and provenance analyses indicate the existence of continent-derived detritus in siliciclastic rocks associated to the arc-related volcanics in correlatable units in Ecuador (Macuchi Arc; Vallejo et al., 2009). These characteristics allow us to consider an Aleutian-type geodynamic setting as a possible scenario for the origin of the Paleocene – Eocene magmatic rocks of the northwestern Andes and Panama, where the arc domain laterally transitioned from a continental to a fully oceanic configuration. Furthermore, the presence of ~67 Ma acidic volcanic rocks, suggest that the Panama Arc magmatism must have initiated earlier than previously considered (~71 Ma, Buchs et al., 2010), since recent chemo-stratigraphic studies of subduction-related rocks, demonstrated that the transition from the eruption of forearc MORB-like basalts to acid calc-alkaline rocks takes ca. 10 m.y (Ishizuka et al., 2014; Whattam and Stern, 2011).

The temporal and geochemical features of the Paleogene tectono-

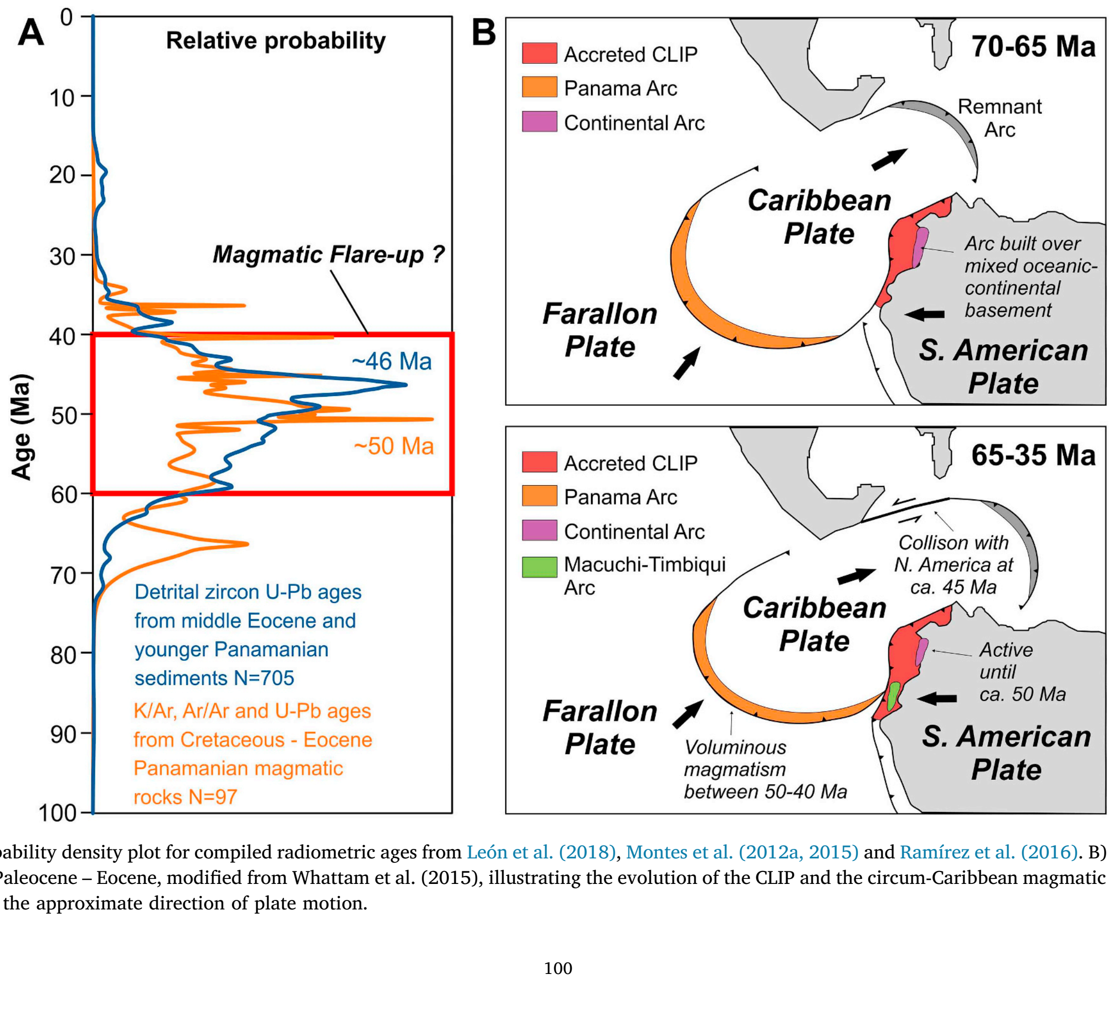

Fig. 12. A) Probability density plot for compiled radiometric ages from León et al. (2018), Montes et al. (2012a, 2015) and Ramírez et al. (2016). B) Paleogeographic scheme for the Paleocene – Eocene, modified from Whattam et al. (2015), illustrating the evolution of the CLIP and the circum-Caribbean magmatic arcs. Large black arrows indicate the approximate direction of plate motion.

magmatic domains exposed in the northern Andes and central-eastern Panama, which were reviewed and discussed above, suggest that they resulted from complex regional-scale plate kinematics that are partially understood. We expect that the compiled geochronological and geochemical data, together with the new results and discussions presented here, constitute a valuable contribution to the understanding of the paleogeography of the circum-Caribbean.

Supplementary data to this article can be found online at https://doi.org/10.1016/j.tecto.2018.10.032.

Acknowledgements

The Smithsonian Tropical Research Institute supported fieldwork in Panama. We appreciate the financial support received from the Fundación para la Promoción de la Investigación y la Tecnología (FPIT) of Banco de la República de Colombia (project 3.809), and from the ACGGP-Ares Corrigan fund granted to S. León. The Colombian Science Foundation (COLCIENCIAS) supported A. Cardona and J. S. Jaramillo (grants 50491 and 51686). Continuous discussion on the Northern Andes Paleogene magmatism with Germán Bayona are deeply acknowledged. Cesar Silva and Marion Weber are also acknowledged for discussion during field sampling of the Panamanian and Colombian plutons. Comments and suggestions by Scott Whattam, an anonymous reviewer and the editorial care of Philippe Agard that improved the quality of the manuscript are deeply acknowledged. Continuous discussion on the Northern Andes Paleogene magmatism with Germán Bayona are deeply acknowledged.

References

Amelin, Y., Lee, D.C., Halliday, A.N., 2000. Early-middle Archaean crustal evolution deduced from Lu-Hf and U-Pb isotopic studies of single zircon grains. Geochim. Cosmochim. Acta 64 (24), 4205–4225.
Anderson, T.A., 1972. Paleogene nonmarine Gualanday Group, Neiva basin, Colombia, and regional development of the Colombian Andes. Geol. Soc. Am. Bull. 83, 2423–2438.
ANH-GRP, 2011. Cartografía Geológica a Escala 1:100.000 de Las Planchas 340, 362, 385 Y 409 Localizadas En La Cuenca Tumaco, Así Como El Inherente Levantamiento de Columnas Estratigráficas Y Muestreo Litológico Para Los Análisis Petrográficos, Bioestratigráficos, geoquímicos, petrofísicos, y radiométricos. Contrato 084 de 2010. (unpublished).
ANH-Universidad de Caldas, 2011. Estudio Geológico Integrado en La Cuenca Tumaco Onshore. Síntesis Cartográfica, Sísmica Y Análisis Bioestratigráfico, Petrográfico, Geocronológico, Termocronológico Y Geoquímico de Testigos de Perforación Y Muestras de Superficie. Informe Final Contrato 092 de 2009. (unpublished).
Annells, R.N., Forero, H.F., Rodríguez, C.A., 1988. Geology and gold potential of the Timbiquí and Napi river basins, Cauca Department, Colombia. In: BGS Technical Report. Ingeominas (WC/88/45, 73 p.).
Aspden, J.A., McCourt, W.J., Brook, M., 1987. Geometrical control of subduction-related magmatism: the Mesozoic and Cenozoic plutonic history of western Colombia. J. Geol. Soc. (Lond.) 144, 893–905. https://doi.org/10.1144/gsjgs.144.6.0893.
Barbosa-Camacho, G., 2003. Memoria Explicativa del Mapa Geológico del Departamento del Cauca: Santiago de Cali, Colombia. Ministerio de Minas y Energía, Instituto de Investigación e Información Geocientífica, Minero-Ambiental y Nuclear (INGEOMINAS) (221 p.).
Bayona, G.A., Montes, C., Cardona, A., Jaramillo, C., Ojeda, G., Valencia, V., Ayala-Calvo, R.C., 2011. Intraplate subsidence and basin filling adjacent to an oceanic arc-continent collision: a case from the southern Caribbean-South America plate margin. Basin Res. 23, 403–422.
Bayona, G., Cardona, A., Jaramillo, C., Mora, A., Montes, C., Valencia, V., Ayala, C., Montenegro, O., Ibañez-Mejia, M., 2012. Early Paleogene magmatism in the northern Andes: insights on the effects of Oceanic Plateau–continent convergence. Earth Planet. Sci. Lett. 331–332, 97–111.
Beaudon, E., Martelat, J.-E., Amórtegui, A., Lapierre, H., Jaillard, E., 2005. Métabasites de la Cordillère Occidentale d'Équateur: témoins d'une racine océanique sous les Andes d'Équateur. C. R. Géosci. 337, 625–634.
Borrero, C., Pardo, A., Jaramillo, C.M., Osorio, J.A., Cardona, A., Flores, A., Echeverri, S., Rosero, S., Garcia, J., Castillo, H., 2012. Tectonostratigraphy of the Cenozoic Tumaco forearc basin (Colombian Pacific) and its relationship with the northern Andes orogenic build up. J. S. Am. Earth Sci. 39, 75–92.
Buchely, F., Parra, E., Castillo, H., González, F., Dávila, C., Romero, O., 2009. Realización de la cartografía geológica y muestreo geoquímico en las planchas 144, 145, 128, 129, 113 y 114. Ingeominas-GRP (163 p.).
Buchs, D.M., Arculus, R.J., Baumgartner, P.O., Baumgartner-Mora, C., Ulianov, A., 2010. Late Cretaceous arc development on the SW margin of the Caribbean Plate: insights from the Golfito, Costa Rica, and Azuero, Panama, complexes. Geochem. Geophys. Geosyst. 11, Q07S24. https://doi.org/10.1029/2009GC002901.
Burke, K., 1988. Tectonic evolution of the Caribbean. Annu. Rev. Earth Planet. Sci. 16 (1), 201–230.
Bustamante, C., Cardona, A., Archanjo, C.J., Bayona, G., Lara, M., Valencia, V., 2017. Geochemistry and isotopic signatures of Paleogene plutonic and detrital rocks of the Northern Andes of Colombia: a record of post-collisional arc magmatism. Lithos 277, 199–209.
Caicedo, J., Roncancio, J., 1994. El Grupo Gualanday como ejemplo de acumulacion sintectonica, en el Valle Superior del Magdalena, durante el Paleogeno. In: Etayo Serna, F. (Ed.), Estudios Geoloicos del Valle Superior del Magdalena. Ecopetrol, Bogota.
Calle, B., Salazar, G., 2007. Geología de la Plancha 185. Ingeominas, Bagadó (Scale 1:100.000, 1 sheet).
Cardona, A., Valencia, V., Weber, M., Duque, J., Montes, C., Ojeda, G., Reiners, P., Domanik, K., Nicolescu, S., Villagómez, D., 2011a. Transient Cenozoic tectonic stages in the southern margin of the Caribbean plate: U-Th/He thermochronological constraints from Eocene plutonic rocks in the Santa Marta massif and Serranía de Jarara, northern Colombia. Geol. Acta 9 (3–4), 445–466.
Cardona, A., Valencia, V.A., Bayona, G., Duque, J., Ducea, M., Gehrels George, E., Jaramillo, C., Montes, C., Ojeda, G., Ruiz, J., 2011b. Early-subduction-related orogeny in the northern Andes; Turonian to Eocene magmatic and provenance record in the Santa Marta Massif and Rancheria Basin, northern Colombia. Terra Nova 23 (1), 26–34.
Cardona, A., Montes, C., Ayala, C., Bustamante, C., Hoyos, N., Montenegro, O., Ojeda, C., Nino, H., Ramirez, V., Valencia, V., Rincon, D., Vervoort, J.D., Zapata, S., 2012. From arc-continent collision to continuous convergence, clues from Paleogene conglomerates along the southern Caribbean-South America plate boundary. Tectonophysics 580, 58–87.
Cardona, A., Weber, M., Valencia, V., Bustamante, C., Montes, C., Cordani, U., Muñoz, C.M., 2014. Geochronology and geochemistry of the Parashi granitoid, NE Colombia: tectonic implication of short-lived Early Eocene plutonism along the SE Caribbean margin. J. S. Am. Earth Sci. 50, 75–92.
Case, J.E., MacDonald, W.D., Fox, P.J., 1990. Caribbean crustal provinces; seismic and gravity evidence. In: Dengo, G., Case, J.E. (Eds.), The Geology of North America. H. Geological Society of America, The Caribbean Region, pp. 15–36.
Chapman, J.B., Ducea, M.N., DeCelles, P.G., Profeta, L., 2015. Tracking changes in crustal thickness during orogenic evolution with Sr/Y: an example from the North American Cordillera. Geology 43 (10), 919–922.
Chauvel, C., Lewin, E., Carpentier, M., Arndt, N.T., Marini, J.C., 2008. Role of recycled oceanic basalt and sediment in generating the Hf–Nd mantle array. Nat. Geosci. 1, 64–67.
Chiaradia, M., 2009. Adakite-like magmas from fractional crystallization and melting-assimilation of mafic lower crust (Eocene Macuchi arc, Western Cordillera, Ecuador). Chem. Geol. 265 (3), 468–487.
Chiaradia, M., 2015. Crustal thickness control on Sr/Y signatures of recent arc magmas: an Earth scale perspective. Sci. Rep. 5, 8115. https://doi.org/10.1038/srep08115.
Closs, M., 1993. Lithospheric buoyancy and collisional orogenesis: subduction of oceanic plateaus, continental margins, island areas, spreading ridges and seamounts. Geol. Soc. Am. Bull. 105, 715–737.
Coates, A.G., Collins, L.S., Aubry, M.P., Berggren, W.A., 2004. The geology of the Darien, Panama, and the late Miocene-Pliocene collision of the Panama arc with northwestern South America. Geol. Soc. Am. Bull. 116 (11–12), 1327–1344.
Corral, I., Cardellach, E., Corbella, M., Canals, A., Gómez-Gras, A.G., Cosca, M.A., 2016. Cerro Quema (Azuero Peninsula, Panama): Geology, alteration, mineralization, and geochronology of a volcanic dome-hosted high-sulfidation Au-Cu deposit. Econ. Geol. 111 (2), 287–310.
Correa, T., Zapata, J.P., Rincón, A.V., Obando, M.J., Ortiz, F.H., Rodriguez, G., 2017. Edades U-Pb y Ar-Ar obtenidas durante la cartografía 1:50.000 del borde occidental de la plancha 130, Medellín Occidental. Memorias XVI Congreso Colombiano de Geología, Santa Marta. pp. 1223–1228.
Davies, J.H., Bickle, M.J., 1991. A physical model for the volume and composition of melt produced by hydrous fluxing above subduction zones. R. Soc. Lond. Philos. Trans. A 335 (1638), 355–364.
Del Giudice, D., Recchi, G., 1969. Geologia del area del Proyecto Minero de Azuero. Informe técnico preparado para el gobierno de la República de Panamá por las Naciones Unidas, actuando y participando como agencia ejecutora. Gobierno de la República de Panamá (48 p.).
Diebold, J., Driscoll, N., 1999. New Insights on the Formation of the Caribbean Basalt Province revealed by Multichannel seismic images of volcanic structures in the Venezuelan basin. In: Sedimentary Basins of the World. 4. pp. 561–589.
Ducea, M., Sen, G., Eiler, J., Fimbres, J., 2002. Melt depletion and subsequent metasomatism in the shallow mantle beneath Koolau volcano, Oahu (Hawaii). Geochem. Geophys. Geosyst. 3 (2), 1–17. https://doi.org/10.1029/2001GC000184.
Ducea, M.N., Paterson, S.R., DeCelles, P.G., 2015. High-volume magmatic events in subduction systems. Elements 11 (2), 99–104.
DuFrane, S.A., Vervoort, J.D., Hart, G.L., 2007. Unertainty of Hf isotope analysis in zircon using LA-MC-ICPMS techniques: full disclosure. In: 17th Annual V.M. Goldschmidt Conference, Cologne, Germany. Geochimica et Cosmochimica Acta 71. pp. A241.
Duque-Caro, H., 1990. Neogene stratigraphy, paleoceanography and paleobiogeography in northwest South America and the evolution of the Panama seaway. Palaeogeogr. Palaeoclimatol. Palaeoecol. 77 (3–4), 203–234.
Echeverri, S., Cardona, A., Pardo-Trujillo, A., Borrero, C., Rosero, S., López, S., 2015a. Correlación y geocronología Ar-Ar del basamento Cretácico y el relleno sedimentario Eoceno superior - Mioceno (Aquitaniano inferior) de la cuenca de antearco de Tumaco, SW de Colombia. Rev. Mex. Cienc. Geol. 32, 179–189.
Echeverri, S., Cardona, A., Pardo, A., Monsalve, G., Valencia, V.A., Borrero, Rosero, S.,

López, S., 2015b. Regional provenance from southwestern Colombia fore-arc and intra-arc basins: implications for Middle to Late Miocene orogeny in the Northern Andes. Terra Nova 27, 356–363. https://doi.org/10.1111/ter.12167.
Echeverri, S., Pardo-Trujillo, A., Borrero, C., Cardona, A., Rosero, S., Celis, S.A., López, S.A., 2016. Estratigrafía del Neógeno Superior al sur de la cuenca Tumaco (Pacífico colombiano): la Formación Cascajal, propuesta de redefinición litoestratigráfica. Bol. Geol. 38 (4), 43–60.
Escalona, A., Mann, P., 2006. An overview of the petroleum system of Maracaibo Basin. AAPG bulletin 90 (4), 657–678.
Escalona, A., Mann, P., 2011. Tectonics, basin subsidence mechanisms, and paleogeography of the Caribbean-South American plate boundary zone. Mar. Pet. Geol. 28, 8–39. https://doi.org/10.1016/j.marpetgeo.2010.01.016.
Farris, D.W., Jaramillo, C., Bayona, B., Restrepo-Moreno, S.A., Montes, C., Cardona, A., Mora, A., Speakman, R.J., Glascock, M.D., Valencia, V., 2011. Fracturing of the Panamanian Isthmus during initial collision with South America. Geology 39 (11), 1007–1010.
Farris, D.W., Cardona, A., Montes, C., Foster, D.A., Jaramillo, C., 2017. Magmatic evolution of Panama Canal volcanic rocks: a record of arc processes and tectonic change. PLoS One 12, e0176010. https://doi.org/10.1371/journal.pone.0176010.
Flinch, J.F., 2003. Structural evolution of the Sinu-Lower Magdalena area (Northern Colombia). In: Bartolini, C., Buffler, R.T., Blickwede, J. (Eds.), The Circum-Gulf of Mexico and the Caribbean: Hydrocarbon Habitats, Basin Formation, and Plate Tectonics. AAPG Memoir 79. pp. 776–796.
Galer, S.J.G., Abouchami, W., 2004. Mass bias correction laws suitable for MC-ICPMS measurement. Geochim. Cosmochim. Acta 68, A542.
Gazel, E., Hayes, J.L., Hoernle, J., Everson, E., Holbrook, S., Hauff, F., van den Bogaard, P., Vance, E.A., Chu, S., Calver, A.J., Carr, M.J., Yogodzinski, G.M., 2015. Continental crust generated in oceanic arcs. Nat. Geosci. 8, 321–327.
George, R., Turner, S., Hawkesworth, C., Morris, J., Nye, C., Ryan, J., Zheng, S.-H., 2003. Melting processes and fluid and sediment transport rates along the Alaska-Aleutian arc from an integrated U-Th-Ra-Be isotope study. J. Geophys. Res. 108, 2252. https://doi.org/10.1029/2002JB001916. (B5).
Gómez, E., Jordan, T.E., Allmendinger, R.W., Hegarty, K., Kelley, S., Heizler, M., 2003. Controls on architecture of the Late Cretaceous to Cenozoic southern Middle Magdalena Valley Basin, Colombia. Geol. Soc. Am. Bull. 115, 131–147.
Gómez-Tapias, J., Montes-Ramírez, M., Nivia, A., Diederix, H., 2015. Mapa Geológico de Colombia. Servicio Geológico Colombiano (scale 1:1000.000, 1 sheet).
Gonzalez, H., 2001. Mapa geológico del Departamento de Antioquia (Memoria explicativa). Ingeominas (240 p.).
González, H., Londoño, A.C., 2002. Catálogo de las unidades litoestratigráficas de Colombia, Batolito de Mandé. Ingeominas, pp. 1–26 ISSN0121-8425.
Herrera, F., Manchester, S., Jaramillo, C., 2012. Permineralized fruits from the late Eocene of Panama give clues of the composition of forests established early in the uplift of Central America. Rev. Paleobot. Palynol. 175, 10–24.
Hincapié-Gómez, S., Cardona, A., Jiménez, G., Monsalve, G., Ramírez-Hoyos, L., Bayona, G., 2018. Paleomagnetic and gravimetrical reconnaissance of Cretaceous volcanic rocks from the Western Colombian Andes: Paleogeographic connections with the Caribbean Plate. Stud. Geophys. Geod. 62 (3), 485–511.
Hughes, R.A., Pilatasig, L.F., 2002. Cretaceous and Tertiary terrane accretion in the Cordillera Occidental of the Andes of Ecuador. Tectonophysics 345 (1–4), 29–48.
Irvine, T.N., Baragar, W.R.A., 1971. A guide to the chemical classification of the common volcanic rocks. Can. J. Earth Sci. 8, 523–548.
Ishizuka, O., Tani, K., Reagan, M.K., 2014. Izu-Bonin-Mariana forearc crust as a modern ophiolite analogue. Elements 10 (2), 115–120.
Iturralde-Vinent, M.A., García-Casco, A., Rojas-Agramonte, Y., Proenza, J.A., Murphy, J.B., Stern, R.J., 2016. The geology of Cuba: a brief overview and synthesis. GSA Today 26 (10), 4–10.
Janoušek, V., Farrow, C.M., Erban, V., 2006. Interpretation of whole-rock geochemical data in igneous geochemistry: introducing Geochemical Data Toolkit (GCDkit). J. Petrol. 47 (6), 1255–1259.
Jaramillo, C., Montes, C., Cardona, A., Silverstro, D., Antonelli, A., Bacon, C.D., 2017. Comment (1) on “Formation of the Isthmus of Panama” by O'dea et al. Sci. Adv. 3, e160231.
Kay, S.M., Godoy, E., Kurtz, A., 2005. Episodic arc migration, crustal thickening, subduction erosion, and magmatism in the south-central Andes. Geol. Soc. Am. Bull. 117, 67–88.
Kerr, A.C., Marriner, G.F., Tarney, J., Nivia, A., Saunders, A.D., Thirlwall, M.F., Sinton, C.W., 1997. Cretaceous basaltic terranes in Western Colombia: elemental, chronological and Sr-Nd isotopic constraints on petrogenesis. J. Petrol. 38, 677–702.
Kerr, A.C., White, R.V., Thompson, P.M.E., Tarney, J., Saunders, A.D., 2003. No oceanic plateau—no Caribbean Plate? The seminal role of an oceanic plateau in Caribbean Plate evolution. In: Bartolini, C., Buffler, R., Blickwede, J. (Eds.), The Circum-Gulf of Mexico and the Caribbean: Hydrocarbon Habitats, Basin Formation and Plate Tectonics. AAPG Memoir 79. pp. 126–168.
Kolarsky, R.A., Mann, P., Monechi, S., 1995. Stratigraphic development of southwestern Panama as determined from integration of marine seismic data and onshore geology. In: Mann, P. (Ed.), Geologic and Tectonic Development of the Caribbean Plate Boundary in Southern Central America. Geological Society of America Special Papers 295. pp. 159–200.
Krawinkel, H., Wozazek, S., Krawinkel, J., Hellmann, W., 1999. Heavy-mineral analysis and clinopyroxene geochemistry applied to provenance analysis of lithic sandstones from the Azuero-Sona Complex (NW Panama). Sediment. Geol. 124 (1–4), 149–168.
Leal-Mejía, H., 2011. Phanerozoic Gold Metallogeny in the Colombian Andes: A Tectonomagmatic Approach (PhD Thesis). University of Barcelona, Barcelona (1000 p.).
Lebras, M., Mégard, F., Dupuy, C., Dostal, J., 1987. Geochemistry and tectonic setting of pre-collision Cretaceous and Paleogene volcanic rocks of Ecuador. Geol. Soc. Am. Bull. 99, 569–578.
León, S., Cardona, A., Parra, M., Sobel, E.R., Jaramillo, J.S., Glodny, J., ... Pardo-Trujillo, A., 2018. Transition from collisional to subduction-related regimes: an example from Neogene Panama-Nazca-South America interactions. Tectonics 37 (1), 119–139. https://doi.org/10.1002/2017TC004785.
Lidiak, E.G., Jolly, W.T., 1996. Circum-Caribbean granitoids: characteristics and origin. Int. Geol. Rev. 38 (12), 1098–1133.
Lissinna, B., 2005. A Profile Through the Central American Landbridge in Western Panama: 155 Ma Interplay Between the Galapagos Hotspot and the Central American Subduction Zone (PhD thesis). Christian-Albrechts University, Kiel (116 p.).
López-Ramos, E., 2009. Evolution tectono-stratigraphique du doble basin avant-arc de la marge convergente Sud Colombienne-Nord Equatorienne pedant le Cenozoique (PhD. Thesis). Universidad de Nice Sophia Antipolis, Nice (349 p.).
Lugo, J., Mann, P., 1995. Jurassic-Eocene tectonic Evolution of Maracaibo basin, Venezuela. In: Tankard, A., Suarez, R., Welsink, H. (Eds.), Petroleum Basins of South America. 62. American Association of Petroleum Geologists Memoir, pp. 699–725.
Mamani, M., Wörner, G., Sempere, T., 2010. Geochemical variations in igneous rocks of the central Andean orocline (13°S to 18°S): tracing crustal thickening and magma generation through time and space. Geol. Soc. Am. Bull. 122, 162–182.
Mann, P., Corrigan, J.C., 1990. Model for Late Neogene deformation in Panama. Geology 18, 558–562.
Mauffret, A., Leroy, S., 1997. Seismic stratigraphy and structure of the Caribbean igneous province. Tectonophysics 283, 61–104.
Maury, R.C., Defant, M.J., Bellon, H., de Boer, J.Z., Stewart, R.H., Cotten, J., 1995. Early Tertiary arc volcanics from eastern Panama. In: Mann, P. (Ed.), Geologic and Tectonic Development of the Caribbean Plate Boundary in Southern Central America: Boulder, Colorado. Geological Society of America Special Paper 295. pp. 29–34.
McCourt, W.J., Aspden, J.A., Brook, M., 1984. New geological and geochronological data from the Colombian Andes: continental growth by multiple accretion. J. Geol. Soc. Lond. 141 (5), 831–845.
McCourt, W., Muñoz, C., Villegas, H., 1990a. Regional geology and gold potential of de Guapi-Napi Drainage basin and upper Timbiquí river. In: Cauca department. SW. Colombia. Valle and Cauca Pacific Coast Precious Metals Project (Phase II). D-425, (75 p.).
McCourt, W.J., Muñoz, U., Villegas, V., 1990b. Regional geology and gold potential of the Guapi–Napi drainage basin and upper Timbiqui river. In: Cauca Department, SW Colombia: British Geological Survey, Overseas Geology Series, Technical Report WC/90/34, (112 p.).
Middlemost, E.A.K., 1994. Naming materials in magma/igneous rock system. Earth Sci. Rev. 37, 215–224.
Montes, C., Guzman, G., Bayona, G., Cardona, A., Valencia, V., Jaramillo, C., 2010. Clockwise rotation of the Santa Marta massif and simultaneous Paleogene to Neogene deformation of the Plato-San Jorge and Cesar-Ranchería basins. J. S. Am. Earth Sci. 29 (4), 832–848.
Montes, C., Cardona, A., McFadden, R., Morón, S.E., Silva, C.A., Restrepo-Moreno, S., ... Bayona, G.A., 2012a. Evidence for middle Eocene and younger land emergence in central Panama: implications for Isthmus closure. Geol. Soc. Am. Bull. 124 (5–6), 780–799.
Montes, C., Bayona, G., Cardona, A., Buchs, D.M., Silva, C.A., Morón, S., ... Valencia, V., 2012b. Arc-continent collision and orocline formation: closing of the Central American seaway. J. Geophys. Res. Solid Earth 117, B04105.
Montes, C., Cardona, A., Jaramillo, C., Pardo, A., Silva, J.C., Valencia, V., Ayala, C., Pérez-Angel, L.C., Rodriguez-Parra, L.A., Ramirez, V., Niño, H., 2015. Middle Miocene closure of the Central American Seaway. Science 348, 226–229.
Mora, A., Baby, P., Roddaz, M., Parra, M., Brusset, S., Hermoza, W., Espurt, N., 2010. Tectonic history of the Andes and sub-Andean zones. In: Hoorn, C., Wesselingh, F.P. (Eds.), Implications for the Development of the Amazon Drainage Basin. Amazonia: Landscape and Species Evolution: A Look Into the Past Blackwell, pp. 38–60.
Moron, S., Fox, D., Feinberg, J., Jaramillo, C., Bayona, G., Montes, C., Bloch, J., 2013. Climate change during the Early Paleogene in the Bogotá Basin (Colombia) inferred from paleosol carbon isotope stratigraphy, major oxides, and environmental magnetism. Palaeogeogr. Palaeoclimatol. Palaeoecol. 388, 115–127.
Nakamura, N., 1974. Determination of REE, Ba, Fe, Mg, Na, and K in carbonaceous and ordinary chondrites. Geochim. Cosmochim. Acta 38, 757–775.
Nie, J., Horton, B.K., Mora, A., Saylor, J.E., Housh, T.B., Rubiano, J., Naranjo, J., 2010. Tracking exhumation of Andean ranges bounding the Middle Magdalena Valley Basin, Colombia. Geology 38 (5), 451–454.
O'Dea, A., Lessios, H.A., Coates, A.G., Eytan, R.I., Restrepo-Moreno, S.A., Cione, A.L., ... Stallard, R.F., 2016. Formation of the Isthmus of Panama. Sci. Adv. 2 (8), e1600883.
Ordoñez, O., Pimentel, M.M., Armstrong, R.A., Gioia, S.M.C.L., Junges, S., 2001. U–Pb SHRIMP and Rb–Sr Ages of the Sonsón Batholith. In: Proceedings, III South-American Symposium on Isotope Geology, Pucon, Chile.
Ordoñez-Carmona, O., Restrepo, J.J., De Brito, R.S.C., Martens, U., Rodrigues, J.B., 2011. The late Paleocene age of the Santa Bárbara Batholith (Valle, Colombia) and its implications on the evolution of the Arquía Complex. In: Proceedings, XIV Congreso Latinoamericano de Geología y XIII Congreso Colombiano de Geología, Medellín Colombia, pp. 109.
Parra, M., Mora, A., Sobel, E.R., Strecker, M.R., González, R., 2009. Episodic orogenic front migration in the northern Andes: Constraints from low-temperature thermochronology in the Eastern Cordillera, Colombia. Tectonics 28, TC4004. https://doi.org/10.1029/2008TC002423.
Pearce, J.A., 1996. A user's guide to basalt discrimination diagrams. In: Wyman, D.A. (Ed.), Trace Element Geochemistry of Volcanic Rocks: Applications for Massive Sulphide Exploration. Geological Association of Canada, Short Courses Notes 12. pp. 79–113.

Pearce, J.A., 2008. Geochemical fingerprinting of oceanic basalts with applications to ophiolite classification and the search for Archean oceanic crust. Lithos 100, 14–48.
Pindell, J.L., Barret, S.F., 1990. Geological evolution of the Caribbean region; a plate-tectonic perspective. In: The Geology of North America. H. The Geological Society of America, The Caribbean Region, pp. 405–432.
Pindell, J.L., Kennan, L., 2009. Tectonic evolution of the Gulf of Mexico, Caribbean and northern South America in the mantle reference frame: an update. In: James, K., Lorente, M.A., Pindell, J. (Eds.), The Geology and Evolution of the Region Between North and South America. Geological Society, London, Special Publications 328. pp. 1–55.
Pindell, J.L., Kennan, L., Maresch, W.V., Stanek, K.P., Draper, G., Higgs, R., 2005. Plate-kinematics and crustal dynamics of circum-Caribbean arc-continent interactions, and tectonic controls on basin development in Proto-Caribbean margins. In: Avé-Lallemant, H.G., Sisson, V.B. (Eds.), Caribbean–South American Plate Interactions, Venezuela. Geological Society of America Special Papers 394. pp. 7–52.
Pindell, J., Maresch, W.V., Martens, U., Stanek, K., 2012. The Greater Antillean Arc: Early Cretaceous origin and proposed relationship to Central American subduction mélanges: implications for models of Caribbean evolution. Int. Geol. Rev. 54 (2), 131–143.
Priem, H.N.A., Beets, D.J., Verdurmen, E.A.T., 1986. Precambrian rocks in an Early Tertiary conglomerate on Bonaire, Netherlands Antilles (southern Caribbean borderland): evidence for a 300 km eastward displacement relative to the South American mainland? Geol. Mijnb. 65, 35–40.
Profeta, L., Ducea, M.N., Chapman, J.B., Paterson, S.R., Henriquez-Gonzales, S.M., Kirsch, M., Petrescu, L., DeCelles, P.G., 2015. Quantifying crustal thickness over time in magmatic arcs. Sci. Rep. 5, 17786. https://doi.org/10.1038/srep17786.
Ramírez, D.A., Foster, D.A., Min, K., Montes, C., Cardona, A., Sadove, G., 2016. Exhumation of the Panama basement complex and basins: implications for the closure of the Central American seaway. Geochem. Geophys. Geosyst. 17 (5), 1758–1777.
Reyes-Harker, A., Ruiz-Valdivieso, C.F., Mora, A., Ramirez-Arias, J.C., Rodriguez, G., de la Parra, F., Caballero, V., Parra, M., Moreno, N., Horton, B.K., Saylor, J.E., Silva, A., Valencia, V., Stockli, D., Blanco, V., 2015. Cenozoic paleogeography of the Andean foreland and retroarc hinterland of Colombia. Am. Assoc. Pet. Geol. Bull. 99, 1407–1453. https://doi.org/10.1306/06181411110.
Rincón, D., Arenas, J.E., Cuartas, C.H., Cardenas, A.L., Molinares, C.E., Caicedo, C., Jaramillo, C., 2007. Eocene-Pliocene planktonic foraminifera biostratigraphy from the continental margin of the southwest Caribbean. Stratigraphy 4, 261–311.
Rodríguez, G., Sierra, M.I., 2010. Las Sedimentitas de Tripogadí y las Brechas de Triganá: Un registro de Volcanismo de Arco, Corrientes de turbidez y levantamiento rápido Eoceno en el noroccidente de Sur América. Geol. Colomb. 35, 74–86.
Rodríguez, G., Zapata, G., 2012. Características del plutonismo Mioceno superior en el segmento norte de la cordillera Occidental e implicaciones tectónicas en el modelo geológico del noroccidente colombiano. Bol. Cienc. la Tierra 31, 5–22.
Rodríguez, G., González, H., Restrepo, J.J., Martens, U., Cardona, J.D., 2012. Ocurrencia de granulitas en el sector septentrional de la cordillera occidental de colombia. Boletín de Geología 34 (2).
Rodríguez, G., Sierra, M.I., Zapata, G., Correa, T., Peláez, J.R., Nivia, A., 2010. Geología de las planchas 58 Sapzurro (Capurganá) 68 Acandí y 79 bis Unguía (Cerro Tagarí, Memorias Explicativas). Ingeominas (246 p.).
Rodriguez-Parra, L.A., Gaitán, C., Montes, C., Bayona, G., Rapalini, A., 2017. Arc-seamount collision: driver for vertical-axis rotations in Azuero, Panama. Stud. Geophys. Geod. 61, 1–20.
Rollins, J., 1965. Stratigraphy and structure of the Guajira Peninsula, northwestern Venezuela and northeastern Colombia. Univ. Nebraska Stud. 30 (102 p.).
Rooney, T.O., Franceschi, P., Hall, C.M., 2010. Water-saturated magmas in the Panama Canal region: a precursor to adakite-like magma generation? Contrib. Mineral. Petrol. 161, 373–388. https://doi.org/10.1007/s00410-010-0537-8.
Ross, P.S., Bédard, J.H., 2009. Magmatic affinity of modern and ancient subalkaline volcanic rocks determined from trace-element discriminant diagrams. Can. J. Earth Sci. 46, 823–839.
Salazar, G., González, L.M., Muñoz, R., Güiza, S., Moreno, J., 2005. Caracterización de unidades litogeoquímicas de la Cordillera Occidental. Ingeominas, Bogotá (82 p.).
Salazar, C.A., Bustamante, C., Archanjo, C.J., 2016. Magnetic fabric (AMS, AAR) of the Santa Marta batholith (northern Colombia) and the shear deformation along the Caribbean Plate margin. J. S. Am. Earth Sci. 70, 55–68.
Sánchez-Celis, D., Frantz, J.C., Charão-Marques, M., Barrera-Cortés, M., 2018. Petrología del Batolito de Acandí y cuerpos asociados, Unguía-Chocó, Colombia. Bol. Geol. 40 (1), 63–81. https://doi.org/10.18273/revbol.v40n1-2018004.
Schütte, P., Chiaradia, M., Beate, B., 2010. Geodynamic controls on Tertiary arc magmatism in Ecuador: constraints from U-Pb zircon geochronology of Oligocene-Miocene intrusions and regional age distribution trends. Tectonophysics 489 (1–4), 159–176.
Seton, M., Müller, R.D., Zahirovic, S., Gaina, C., Torsvik, T., Shephard, G., ... Chandler, M., 2012. Global continental and ocean basin reconstructions since 200 Ma. Earth Sci. Rev. 113 (3–4), 212–270.
Sun, S.S., McDonough, W.S., 1989. Chemical and isotopic systematics of oceanic basalts: implications for mantle composition and processes. Geol. Soc. Lond. Spec. Publ. 42, 313–345.
Tatsumi, Y., Eggins, S., 1995. Subduction Zone Magmatism. vol. 1 Wiley.
Tetreault, J.Á., Buiter, S.J.H., 2012. Geodynamic models of terrane accretion: testing the fate of island arcs, oceanic plateaus, and continental fragments in subduction zones. J. Geophys. Res. Solid Earth 117 (B8).
Thompson, P.M.E., Kempton, P.D., White, R.V., Saunders, A.D., Kerr, A.C., Tarney, J., Pringle, M.S., 2004. Elemental, Hf–Nd isotopic and geochronological constraints on an island arc sequence associated with the Cretaceous Caribbean plateau: Bonaire, Dutch Antilles. Lithos 74 (1), 91–116.
Timm, C., Davy, B., Haase, K., Hoernle, K.A., Graham, I.J., De Ronde, C.E., ... Seebeck, H.C., 2014. Subduction of the oceanic Hikurangi Plateau and its impact on the Kermadec arc. Nat. Commun. 5, 4923.
Vallejo, C., Winkler, W., Spikings, R.A., Luzieux, L., Heller, F., Bussy, F., 2009. Mode and timing of terrane accretion in the forearc of the Andes in Ecuador. In: Kay, S.M., Ramos, V.A., Dickinson, W.R. (Eds.), Backbone of the Americas: Shallow Subduction, Plateau Uplift, and Ridge and Terrane Collision. Geological Society of America Memoir 204. pp. 197–216.
Vervoort, J.D., Blichert-Toft, J., 1999. Evolution of the depleted mantle: Hf isotope evidence from juvenile rocks through time. Geochim. Cosmochim. Acta 63 (3–4), 533–556.
Vervoort, J.D., Patchett, P.J., 1996. Behavior of hafnium and neodymium isotopes in the crust: constraints from Precambrian crustally derived granites. Geochim. Cosmochim. Acta 60 (19), 3717–3733.
Vervoort, J.D., Patchett, P.J., Blichert-Toft, J., Albarède, F., 1999. Relationships between Lu–Hf and Sm–Nd isotopic systems in the global sedimentary system. Earth Planet. Sci. Lett. 168 (1), 79–99.
Vervoort, J.D., Patchett, P.J., Söderlund, U., Baker, M., 2004. Isotopic composition of Yb and the determination of Lu concentrations and Lu/Hf ratios by isotope dilution using MC-ICPMS. Geochem. Geophys. Geosyst. 5, Q11002. https://doi.org/10.1029/2004GC000721.
Villagómez, D., Spikings, R., Magna, T., Kammer, A., Winkler, W., Beltrán, A., 2011. Geochronology, geochemistry and tectonic evolution of the Western and Central cordilleras of Colombia. Lithos 125, 875–896.
Vogt, K., Gerya, T.V., 2014. From oceanic plateaus to allochthonous terranes: numerical modelling. Gondwana Res. 25 (2), 494–508.
Wagner, L.S., Jaramillo, J.S., Ramírez-Hoyos, L.F., Monsalve, G., Cardona, A., Becker, T.W., 2017. Transient slab flattening beneath Colombia. Geophys. Res. Lett. 44, 6616–6623. https://doi.org/10.1002/2017GL073981.
Wegner, W., Wörner, G., Harmon, R.S., Jicha, B.R., 2011. Magmatic history and evolution of the Central American Land Bridge in Panama since Cretaceous times. Geol. Soc. Am. Bull. 123 (3–4), 703–724.
Wetmore, P.H., Ducea, M.N., 2011. Geochemical evidence of a near-surface history for source rocks of the central Coast Mountains Batholith, British Columbia. Int. Geol. Rev. 53 (2), 230–260.
Whattam, S.A., Stern, R.J., 2011. The "subduction initiation rule": a key for linking ophiolites, intra-oceanic forearcs, and subduction initiation. Contrib. Mineral. Petrol. 162, 1031–1045. https://doi.org/10.1007/s00410-011-0638-z.
Whattam, S.A., Stern, R.J., 2015. Late Cretaceous plume-induced subduction initiation along the southern margin of the Caribbean and NW South America: the first documented example with implications for the onset of plate tectonics. Gondwana Res. 27 (1), 38–63.
Whattam, S.A., Montes, C., Mcfadden, R.R., Cardona, A., Ramirez, D., Valencia, V., 2012. Age and origin of earliest adakitic-like magmatism in Panama: implications for the tectonic evolution of the Panamanian magmatic arc system. Lithos 142–143, 226–244. https://doi.org/10.1016/j.lithos.2012.02.017.
Winchester, J.A., Floyd, P.A., 1977. Geochemical discrimination of different magma series and their differentiation products using immobile elements. Chem. Geol. 20, 325–343.
Woodring, W.P., 1964. Geology and paleontology of Canal Zone and adjoining parts of Panama; description of Tertiary mollusks; Gastropods, Columbellidae to Volutidae. U. S. Geol. Surv. Prof. Pap. 0306-C.
Wörner, G., Harmon, R., Wegner, W., 2009. Geochemical evolution of igneous rock and changing magma sources during the formation and closure of the Central American land bridge of Panama. In: Kay, S.M., Ramos, V.A., Dickinson, W.R. (Eds.), Backbone of the Americas: Shallow Subduction, Plateau Uplift, and Ridge and Terrane Collision. Geological Society of America Memoir 204. pp. 183–196. https://doi.org/10.1130/2009.1204(08.
Xie, X.Y., Mann, P., Escalona, A., 2010. Regional provenance study of Eocene clastic sedimentary rocks within the South America-Caribbean plate boundary zone using detrital zircon geochronology. Earth Planet. Sci. Lett. 291 (1–4), 159–171.
Yogodzinski, G.M., Vervoort, J.D., Brown, S.T., Gerseny, M., 2010. Subduction controls of Hf and Nd isotopes in lavas of the Aleutian island arc. Earth Planet. Sci. Lett. 300, 226–238. https://doi.org/10.1016/j.epsl.2010.09.035.
Zapata, G., Rodríguez, G., 2011. Basalto de El Botón, Miocene volcanic arc of Shoshonitic affinity to the North of Cordillera Occidental of Colombia. Bol. Cienc. Tierra 30, 77–92.
Zapata, S., Cardona, A., Montes, C., Valencia, V., Vervoort, J., Reiners, P., 2014. Provenance of the Eocene Soebi Blanco formation, Bonaire, Leeward Antilles: Correlations with post-Eocene tectonic evolution of northern South America. J. S. Am. Earth Sci. 52, 179–193.
Zellmer, G.F., 2008. Some first order observations on magma transfer from mantle wedge to upper crust at volcanic arcs. In: Annen, C. (Ed.), Dynamics of Magma Ascent, Storage and Differentiation. Geological Society, London, Special Publications 304. pp. 15–31.
Zimmer, M.M., Plank, T., Hauri, E.H., Yogodzinski, G.M., Stelling, P., Larsen, J., ... Nye, C.J., 2010. The role of water in generating the calc-alkaline trend: new volatile data for Aleutian magmas and a new tholeiitic index. J. Petrol. 51 (12), 2411–2444.